Contents lists available at ScienceDirect

Palaeogeography, Palaeoclimatology, Palaeoecology

journal homepage: http://ees.elsevier.com

High-resolution stable isotope profiles of modern elephant (*Loxodonta africana*) tusk dentin and tail hair from Kenya: Implications for identifying seasonal variability in climate, ecology, and diet in ancient proboscideans

Kevin T. Uno [a,1,*], Daniel C. Fisher [b], Gerard Schuster [c], George Wittemyer [d,e], Iain Douglas-Hamilton [e,f], Patrick Omondi [g], Moses Litoroh [g], Thure E. Cerling [a,h]

[a] Department of Geology and Geophysics, University of Utah, Salt Lake City, UT 84112, USA
[b] Museum of Paleontology and Department of Earth and Environmental Sciences, University of Michigan, Ann Arbor, MI 48109-1085, USA
[c] King Abdullah University of Science and Technology, Thuwal 23955-6900, Saudi Arabia
[d] Department of Fish, Wildlife and Conservation Biology, Colorado State University, Fort Collins, CO 80523, USA
[e] Save the Elephants, P.O. Box 54667, Nairobi 00200, Kenya
[f] Department of Zoology, Oxford University, Oxford OX1 3PS, United Kingdom
[g] Kenya Wildlife Services, P.O. Box 40241, Nairobi 00100, Kenya
[h] Department of Biology, University of Utah, Salt Lake City, UT 84112, USA

ARTICLE INFO

Keywords
Ivory
Carbon
Oxygen
Paleoecology
Life history
Histology

ABSTRACT

Stable isotope ratios in tissues of large mammalian herbivores record diet and climate information integrated over large spatial areas and can be used to study modern and fossil ecosystems. Sound interpretation of data requires that tissue growth rates be determined accurately and that ecological and behavioral variables that influence stable isotope ratios of tissues be measured and related to experienced environmental conditions assessed through field observations, remote sensing data, and meteorological records. If well-understood in modern herbivores, stable isotopes from closely-related extinct taxa have tremendous potential for resolving paleodiet, paleoenvironment, and paleoclimate of terrestrial ecosystems. We present multiyear, high-resolution (i.e., weekly) stable isotope records from bioapatite in tusk dentin ($\delta^{13}C_{dentin}$ and $\delta^{18}O_{dentin}$) and tail hair ($\delta^{13}C_{hair}$ and $\delta^{15}N_{hair}$) of an African elephant (*Loxodonta africana*) from Kenya that was fitted with a GPS collar intermittently over a five year period and observed for nearly a decade. GPS and observational data provide behavioral, life history, and location information. Normalized Difference Vegetation Index (NDVI), precipitation, and isotopic data from plants and water provide further constraints for interpreting isotope profiles. We determine tusk and hair growth rates using a combination of histological and geochemical approaches, including bomb-curve radiocarbon, that confirm approximately weekly resolution in the stable isotope profiles. Tusk dentin isotope profiles spanning the periods 1982 to 1987 and 2000 to 2006 record weekly variability in $\delta^{13}C_{dentin}$, where increases of up to 4.5‰ from baseline values due to diet switches from predominantly C_3 browsing to mixed C_3 browsing and C_4 grazing occur during the twice-yearly (biannual) rainy seasons. The $\delta^{13}C_{hair}$ values show a similar trend. The $\delta^{13}C$ profiles served as a proxy for seasonal changes in rainfall, vegetation, and diet. The $\delta^{18}O$ of tusk bioapatite varied approximately biannually up to 5‰, likely reflecting increases in the proportion of plant water ingested during the wet season. Using a least squares inverse filter, we show that NDVI can be used to predict $\delta^{13}C$ of dentin and vice versa, offering the possibility to reconstruct seasonal changes in vegetation and rainfall in the geologic past. Our results demonstrate that high-resolution tusk isotope profiles serve as a proxy for seasonality of diet and precipitation, and thus can be used to reconstruct aspects of elephant life history, vegetation, and climate at unprecedented resolution from modern and fossil proboscidean samples.

* Corresponding author.
E-mail addresses: kevinuno@ldeo.columbia.edu (K.T. Uno); dcfisher@umich.edu (D.C. Fisher); gerard.schuster@kaust.edu.sa (G. Schuster); G.Wittemyer@ColoState.edu (G. Wittemyer); iain@savetheelephants.org (I. Douglas-Hamilton); pomondi@kws.go.ke (P. Omondi); thure.cerling@utah.edu (T.E. Cerling)
[1] Current affiliation is Division of Biology and Paleo Environment, Lamont-Doherty Earth Observatory of Columbia University, Palisades, NY 10964, United States of America.

https://doi.org/10.1016/j.palaeo.2020.109962
Received 23 May 2020; Received in revised form 8 August 2020; Accepted 8 August 2020
Available online xxx
0031-0182/

1. Introduction

The utility of stable isotopes in modern and paleoecological studies has been an area of active research since the pioneering work on stable isotopes as tracers in plant and herbivore ecosystems (e.g., DeNiro and Epstein, 1978, 1981; Park and Epstein, 1960; Tieszen et al., 1979). Later studies on carbon, nitrogen, and oxygen isotopes in different animal tissues such as collagen, bioapatite, and keratin provided greater insight into how animal tissues record dietary and climate information (Ambrose and Norr, 1993; Cerling and Harris, 1999; Kohn, 1996; Lee-Thorp et al., 1989; Levin et al., 2006; Podlesak et al., 2008; Tieszen et al., 1983). These advances have led to the widespread use of isotopes to study animal diets and migration patterns as well as climate in modern and ancient ecosystems (e.g., Cerling et al., 2010; Gannes et al., 1998; Hobson, 1999; Secord et al., 2012; Zazzo et al., 2000).

Within the last 30 years, it was recognized that metabolically inert tissues could be serially sampled to provide a time series of stable isotope data. One of the first applications of this method in terrestrial ecosystems was oxygen isotope analysis of dentin bioapatite on late Pleistocene proboscidean tusks and bear canines (Koch et al., 1989). The study demonstrated that stable isotope profiles can be used to evaluate seasonality, and in that particular study, the results were used to determine season of death and to provide additional confirmation for circaseptan periodicities of growth increments in proboscidean tusk and molar dentin. Subsequent studies utilizing isotope profiles from proboscidean tusks and teeth have expanded to include carbon to evaluate diet (e.g., Codron et al., 2012; Fox and Fisher, 2004) and nitrogen to explore weaning and diet (e.g., Metcalfe et al., 2010; Rountrey et al., 2007), and thus give additional information on life history and seasonality of diet, ecology, and climate. Previously published isotope profiles from proboscidean tusk records have a resolution of approximately 2–10 samples per year (e.g., Koch et al., 1989; Fisher and Fox, 2003; Rountrey et al., 2007; Codron et al., 2012; and Cherney et al., 2017), which is sufficient for detecting annual periodicities in diet and climate signals. However, for higher frequency changes in diet or climate, such as the twice-yearly (biannual) wet seasons that occur in parts of East Africa today, that resolution may not capture the range and nature of variability according to Nyquist sampling theory (Nyquist, 1928).

African elephant (*Loxodonta africana*) tail hair isotope profiles sampled at approximately weekly resolution captured dietary switches that are a result of biannual wet seasons in Kenya, and the results have implications for understanding elephant ecology and conservation (Cerling et al., 2004; Cerling et al., 2009; Cerling et al., 2006). Tail hair is limiting in that a single hair usually only represents a year's time, and less than 3 years at best. Furthermore, most hair and other keratinous tissues studied to date are collected from an immobilized or recently deceased animal and are rarely preserved after death (cf. Metcalfe, 2018), which precludes obtaining high-resolution isotope profiles from the recent and geologic past.

High-resolution serial sampling of tusks offers an alternative to the relatively short time represented in hair and its paucity in the recent and geologic past. Proboscidean tusks record decades of climate, diet, and life history information (Uno et al., 2020; Uno et al., 2013). Stable isotope profiles from recent and unaltered fossil tusks can be serially sampled at high resolution to provide records of life history and seasonal changes in diet, vegetation, and climate in unprecedented detail and duration. These profiles have the potential to elucidate the frequency and relative intensity of seasonal environmental variability (e.g., in vegetation or precipitation) in ancient ecosystems at a resolution that cannot be obtained from other isotopic proxies such as soil carbonates or plant biomarkers, or other environmental proxies such as pollen, phytoliths, paleosols, or charcoal.

Here we present two carbon and oxygen isotope profiles sampled at approximately weekly resolution from an African elephant tusk. The profiles span the periods 1982 to 1987 and 2000 to 2006. We also present carbon and nitrogen isotope profiles from tail hair from the same individual spanning most of the period from 2000–2006. Using the synchronous hair and tusk profiles, we show for the first time that carbon isotope ratios in hair and tusk provide nearly identical records of diet variability related to seasonal rains. The relationship between biannual wet seasons and diet change, whereby consumption of C_4 vegetation increases from a baseline of 10 to 20% of total diet during the dry season to up to *ca.* 70% during the wet season, is supported by extensive NDVI, GPS, and precipitation data sets. We apply a least squares inverse filter to show that diet (as $\delta^{13}C$) can be reconstructed from NDVI and vice versa using tusk profile data from 1982 to 1987. Our results illustrate the potential use of high-resolution stable isotope profiles for studying the life history of proboscideans and the seasonality of climate variables in modern and ancient terrestrial ecosystems.

2. Background and materials

2.1. Study area and sample collection

Tusk dentin and tail hair sampled for stable isotope analysis come from a single individual, Amina (R37), who was the matriarch of an elephant family unit called the Swahilis. The Swahilis inhabit the Samburu and Buffalo Springs National Reserves (the Reserves) and surrounding area in northern Kenya (Fig. 1; Wittemyer, 2001). The Reserves, located at 0.5° N, 37.5° E, range in elevation from 800–1200 m, cover ~330 km^2 in the Samburu-Laikipia region, and provide a safe haven for the largest population of elephants living outside of protected areas in Kenya (Wittemyer et al., 2013). The primary source of water in the Reserves is the semipermanent Ewaso Ng'iro River and its tributaries; the vegetation communities vary from Acacia (*Vachellia* spp.) and doum palm-dominated forests along the riparian corridors to *Vachellia-Commiphora* semiarid bushlands and *Vachellia* wooded grasslands in the drier regions (Cerling et al., 2009; Wittemyer, 2001).

Using the tooth wear age criteria established by Laws (1966) and refined by Lee et al. (2012), the estimated age of R37 at death was 53 ± 5 years old. Five tail hairs were collected from R37 between January 2001 and September 26, 2006, when the elephant died of what we presume to be natural causes. Tail hair was usually collected opportunistically, during immobilization events for fitting of a GPS collar or later, when changing the battery on the collar. Individual hairs

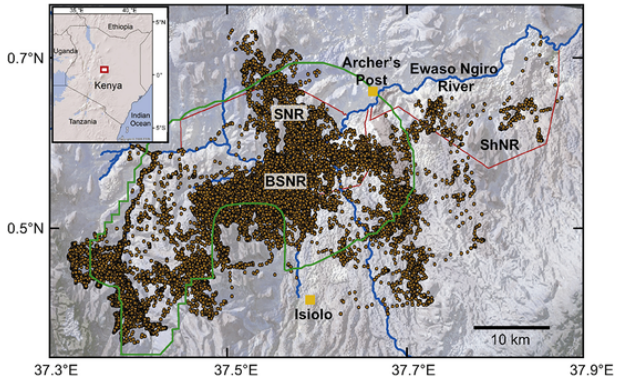

Fig. 1. Schematic map of area occupied by R37 in northern Kenya. Dots indicate hourly GPS locations of R37 between 2001 and 2006. Normalized Difference Vegetation Index data come from the area within the green polygon. Base map from ESRI and inset from Wittemyer et al. (2013). Abbreviations: SNR = Samburu National Reserve; BSNR = Buffalo Springs National Reserve; ShNR = Shaba National Reserve. The border between SNR and BSNR is the Ewaso Ng'iro River. Rainfall data were collected at Archer's Post by the East African Meteorological Department. (For interpretation of the references to colour in this figure legend, the reader is referred to the web version of this article.)

were pulled from the tail with the root end intact so that the proximal end could be easily identified. Hairs ranged in length from 235 to 330 mm.

Within several days of the elephant's death on September 26, 2006, the tusks were removed by Kenya Wildlife Services (KWS) staff and transferred to a KWS ivory strong room in Isiolo, Kenya. The right tusk, the longer of the two and measuring 130 cm from the tip to the pulp cavity margin, was selected for study. In the summer of 2007, the tusk was prepared at a KWS facility in Nairobi for import to the United States (US). According to the terms in the import permit granted by the Convention on International Trade of Endangered Species (CITES) and the US Fish and Wildlife Service, the tusk was to be imported into the US in no more than 20 slabs measuring approximately 4x6x1 cm. The tusk was cross-cut (i.e., transversely) with a bow saw into several segments. Tusk segments were then cut longitudinally, approximately parallel to the structural axis of the tusk (Fig. 2). A second longitudinal cut was made parallel to the first one on each cross-cut segment in order to isolate ~1-cm-thick pieces. Each piece was then cut into smaller slabs that were approximately 4 cm in height, measured radially from the tusk axis to the outer margin, and 4 to 7 cm in length, measured along the tusk axis (Fig. 3A).

2.2. Stable isotopes in plants, water, and elephant tissues

2.2.1. Carbon isotopes

In the semi-arid ecosystem of the Reserves, nearly all species of woody vegetation use the C_3 photosynthetic pathway whereas grasses and at least one shrub, *Salsola denroides*, employ the C_4 photosynthetic pathway. The carbon isotope ratios of C_3 and C_4 plants differ, where C_3 plants typically range from about −30 to −20‰ and C_4 grasses range from about −14 to −10‰ (Cerling and Harris, 1999). The isotopic difference between C_3 and C_4 plants can be traced through the diet of elephants as dietary carbon is incorporated in tusk dentin and hair (Koch et al., 1989; Cerling et al., 2006). The carbon isotope values of these tissues therefore reflect the proportion of C_3 and C_4 resources in elephant diet. Carbon undergoes isotopic enrichment and we use enrichment factors between diet and tissue of +14.1‰ for dentin and +3.1‰ for hair (See Supplementary Text for details).

2.2.2. Hydrogen and oxygen isotopes

Stable oxygen and hydrogen isotopes in animal tissues reflect environmental water and can be used to understand water use, climate, and migration in modern and past ecosystems (e.g., Bowen et al., 2005; Koch et al., 1989). Animals obtain environmental water, which is the dominant source of oxygen and hydrogen in body water, by drinking surface water or ingesting food-bound water (e.g., plant water) (Podlesak et al., 2008). In the Reserves, elephants' drinking water comes from local surface water—namely the Ewaso Ng'iro River and its tributaries, but also ephemeral pools in the wet season—which are fed by local precipitation. Plant water also comes from local precipitation, but in semi-arid ecosystems, it is isotopically enriched in ^{18}O and deuterium compared to precipitation and river water due to the combined effects of soil water and leaf water evaporation (Cernusak et

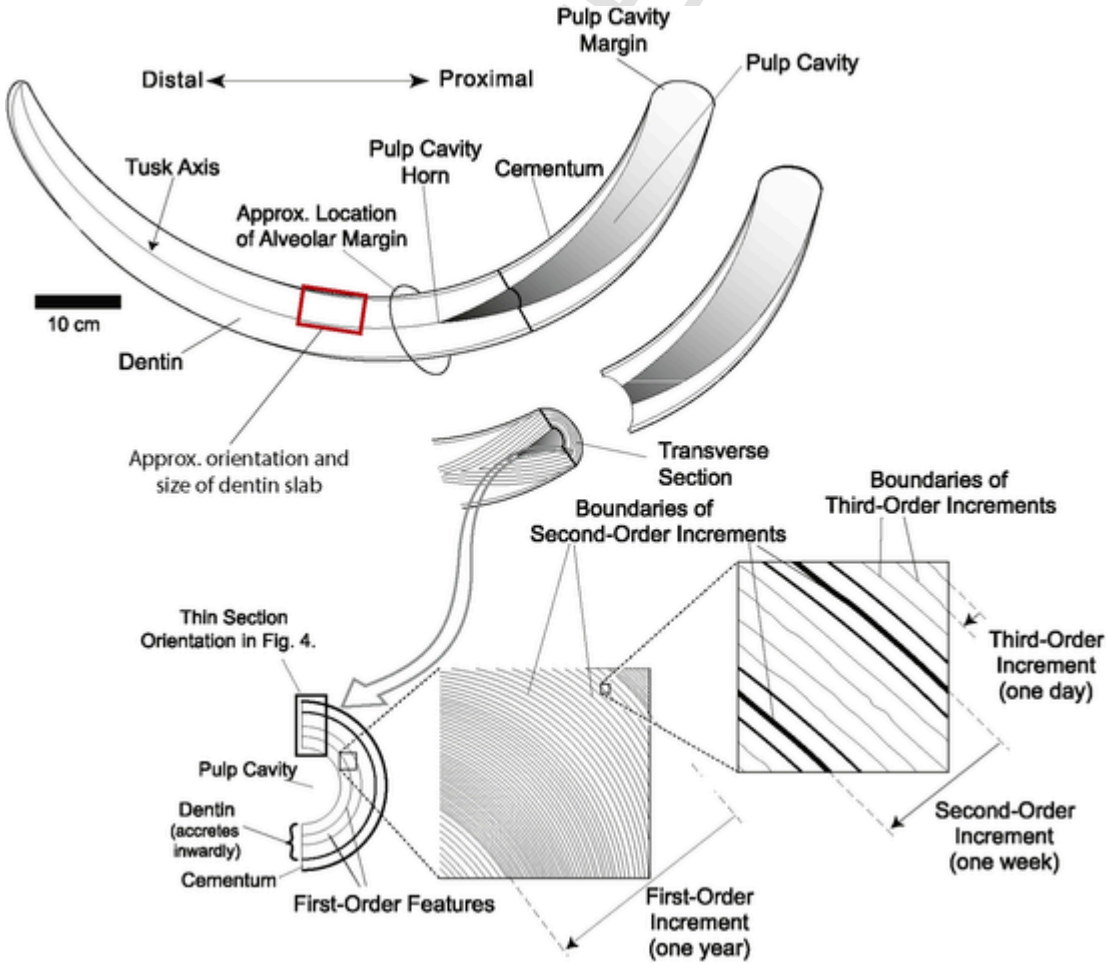

Fig. 2. Schematic illustrating structural features and periodic growth increments in a tusk of an elephant (*Loxodonta africana*). Upper: longitudinally-cut elephant tusk showing structural features and approximate size and orientation of tusk dentin slabs (red outline); Lower: transverse view illustrating first-, second-, and third-order growth increments. Modified from Fisher and Fox (2007). (For interpretation of the references to colour in this figure legend, the reader is referred to the web version of this article.)

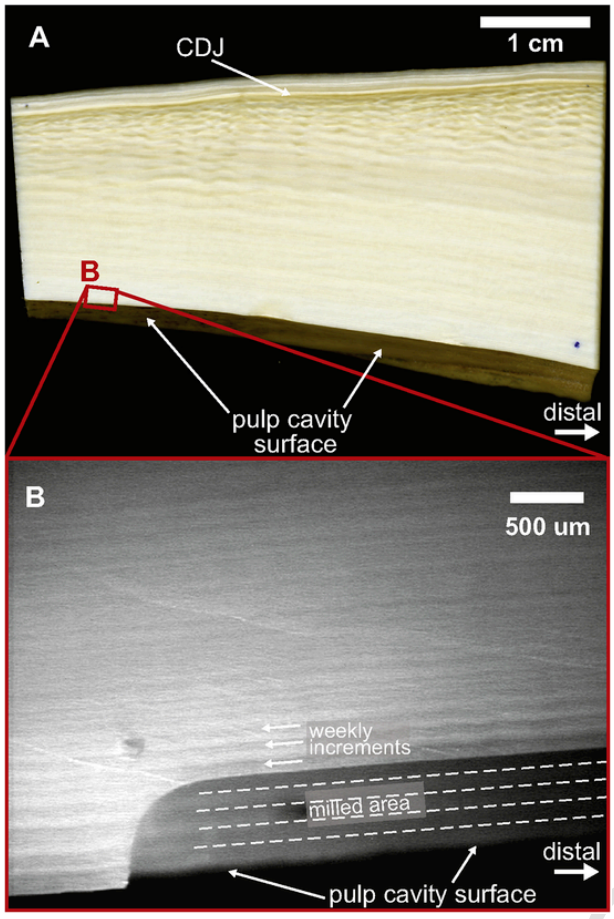

Fig. 3. A) Photograph of the polished longitudinal surface of tusk dentin slab 1169 prior to serial sampling. B) Photomicrograph of the polished longitudinal surface of slab 1169 under reflected light at 40x magnification. Five samples have been milled to a depth of 1000 μm and ~100 μm thickness each, and boundaries are shown with dashed white lines. Approximately weekly increments are indicated by white arrows on the polished tusk dentin surface.

al., 2016). The isotope ratio of elephant body water is recorded in tusk dentin (oxygen) and hair (hydrogen), although dietary protein also contributes to hydrogen in hair (Koch et al., 1989; Ehleringer et al., 2008; Bowen et al., 2005; Cerling et al., 2009). The distinctly more positive isotope ratios in plant water compared to river water provide a means to detect changes in the proportion of these sources in elephant body water. Because elephant body water has a half-life of ~8 days (Uno et al., 2020), isotopes in tusk dentin and hair can be used to track changes in body water resulting from seasonal variability in environmental waters that reflect climate or in proportions of ingested water (e.g., plant versus drinking water) that reflect behavior. Combining these data with auxiliary data, such as GPS tracking, carbon isotopes, or NDVI, will allow us to parse out environmental vs. behavioral influences.

2.3. Structure and composition of tusk dentin

Elephant tusks are highly modified, continuously growing upper incisors comprised primarily of dentin with an outer layer of cementum (Fig. 2). Initially at eruption, the cementum layer is several millimeters thick, but it is usually missing at the distal end of the tusk due to normal wear. Enamel is present only on the bicuspid tip of a tusk when it initially erupts, and is rarely if ever present in tusks of adults. The boundary between the cementum and dentin in a tusk is called the cementum-dentin junction (CDJ) (Fig. 3A). Elephant tusk dentin is comprised of inorganic and organic components, similar to tooth dentin in other mammals. These include hydroxylapatite (~74%), type I collagen (~18%) and other proteins (~3%), and water (~5%) (Williams and Elliott, 1979). In biological hydroxylapatite ($Ca_{10}(PO_4)_6OH$, the carbonate anion (CO_3^{2-}) can substitute in the phosphate (PO_4) or the hydroxyl (OH) positions (Elliott, 2002; LeGeros et al., 1969). Tusk dentin is deposited throughout life along the conical pulp cavity surface, and incremental growth features representing annual, approximately weekly (or for some species, fortnightly), and daily intervals are present in proboscidean tusks. These increments are referred to as first-, second-, and third-order increments (Fig. 2; Fisher, 1996). A geometric analogy for tusk growth is a stack of cones, where a new "cone" (or dentin layer), is added daily at the base of the stack. Detailed discussions of tusk growth processes, incremental growth features, and life history events recorded in tusks can be found in many of Fisher's works (e.g., Fisher, 1996, 2001; Fisher and Fox, 2003, 2007).

2.4. Observational, meteorological, and remote sensing data

Observational, meteorological, and remote sensing data provide a framework of behavioral, life history, climatic, and location information necessary to interpret the stable isotope profiles from tusks and tail hair. From November of 1997 to July 1999, daily observational transects, primarily along water courses in and near the Reserves, were conducted identifying 767 individual elephants in the area (Wittemyer, 2001), and observational transects continue to date with the support of Save the Elephants staff. Field observational data for R37 are detailed in the Supplementary Information and include known and inferred calving events and feeding observations. Using data from GPS collars and field observations, Wittemyer and Getz (2007) determined the rank of 20 family unit matriarchs in and around the Reserves; R37's rank of 13th classified her as mid-low in the social hierarchy and as a result, she had a larger home range than higher ranking matriarchs (549 km^2, LoCoH method), spent less time in protected areas (i.e., the Reserves) than individuals with higher social rank, and had no core area in the Reserves (Wittemyer et al., 2007).

Daily precipitation records spanning the study interval (1982–2006) come from measurements made at Archer's Post (Fig. 1). The region experiences biannual wet seasons that are broadly associated with the movement of the tropical rain belt (Nicholson, 2018). The majority of annual precipitation occurs during the two wet seasons, referred to as the "long rains" (March–May) and the "short rains" (October–December).

Remote sensing products include GPS locational data for R37 and vegetation data collected by satellite. The use of GPS collars to track the location and movement of elephants provides more information than traditional radio collar methods (Douglas-Hamilton, 1998; Douglas-Hamilton et al., 2005). R37 was fitted with a GPS collar that recorded her location at 1 to 3 h intervals for a nearly continuous period from 2001 through September 2006.

Normalized Difference Vegetation Index (NDVI) derived from imagery provided by the National Oceanic and Atmospheric Administration Advanced Very High-resolution Radiometer (AVHRR) satellite (1982–1986) and the Satellite Pour l'Observation de la Terre (SPOT; 2000–2006) were used as a proxy for net primary productivity (NPP) (Supplementary Information; Pettorelli et al., 2005). NDVI data are summed over an area defined by a polygon that circumscribes nearly all GPS and observational location data for elephants using the Reserves (Fig. 1).

3. Methods

This study employs a wide range of methods. Histological analysis of thin sections, sampling of tail hair for isotopic analysis, and isotopic analysis are briefly summarized here and detailed descriptions of

the methods are provided in the Supplementary Information. The more novel approaches of sampling tusk dentin and applying the least squares inverse filter are described more fully herein.

3.1. Sample preparation of ivory for histological analysis

We prepared polished longitudinal surfaces and corresponding thin sections from multiple dentin slabs cut from R37's tusk. Tusk orientations are described in Fig. 2. Polished longitudinal surfaces were used to map out stable isotope sampling plans at weekly resolution, whereas thin sections enabled histological analyses, accomplished through photomicroscopy and image analysis, to determine growth rates. In this study we focus on the three tusk dentin slabs (1169, 1053, and 412) and their corresponding thin sections. Descriptions of sample preparation, imaging, and analysis are provided in the Supplemental Information.

3.2. Sample preparation for stable isotope analysis

3.2.1. Tusk dentin

Tusk dentin was acquired for stable isotope analyses by serial sampling parallel to second-order growth increments in tusk dentin slabs (Fig. 3B). This approach was designed to minimize time averaging that results from sampling across growth increments, which represent approximately weekly isochrons in the tusk. Sequential sampling was carried out using an end-milling technique on a high-precision milling device (Merchantek Micromill). End-milling is described in the Supplementary Information. In summary, 100 μm wide samples were drilled at a depth of 1 mm parallel to growth increments for ~4.5 cm along a longitudinally cut surface of tusk dentin slabs (Fig. 3). The orientation of the slabs is shown as a red box in the tusk schematic in Fig. 2. A total of 639 samples were milled from three tusk dentin slabs (R37-DEN-1169, −1053, and −412). Tusk dentin slab R37-DEN-1169 (slab 1169) comes from the tip of the pulp cavity and 116.9 cm from the distal end of the tusk. Slab 1053 is adjacent to 1169 and was sampled to overlap and extend the record from slab 1169. Slab 412 comes from the distal half of the tusk, 41.2 cm from the tip.

3.2.2. Tail hair

Consecutively formed sample masses of about 500 μg were removed at intervals located every 5 mm along intact hairs, following the methods of Cerling et al. (2009). Additional details are provided in the Supplementary Information.

3.3. Stable isotope analysis

The carbonate component of hydroxylapatite in tusk dentin was analyzed for stable carbon and oxygen isotope ratios by dual-inlet isotope ratio mass spectrometry (IRMS). Tusk dentin samples were first pretreated with an oxidizer (30% H_2O_2) to remove organics (Supplementary Information). Stable isotope ratios are reported as δ-values relative to the Vienna Pee Dee Belemnite (VPDB) scale using permil (‰) notation where.

$$\delta^{13}C\ (\delta^{18}O) = \left(R_{sample}/R_{standard} - 1\right) \quad (1)$$

and R_{sample} and $R_{standard}$ are the $^{13}C/^{12}C$ ($^{18}O/^{16}O$) ratios in the sample and in the standard, respectively, and the $\delta^{13}C$ ($\delta^{18}O$) value of VPDB is defined as 0‰. Internal laboratory standards of tusk dentin (R37-DEN), modern enamel (MCM), and calcium carbonate (UU Carrara) were used for data correction and had average standard deviations of ~0.1‰ for $\delta^{13}C$ and ~0.2‰ for $\delta^{18}O$ across all analytical runs. Standard reference values are given in the *Supplemental Information*.

Tail hair was analyzed for stable carbon and nitrogen isotope ratios, reported as δ-values relative to standards (VPDB for carbon, AIR standard for nitrogen) using permil notation defined in Eq. (1). Analysis was by elemental analyzer-IRMS. The average standard deviation of the standard, SIRFER yeast, pooled from all runs for the five tail hairs is 0.15‰ for $\delta^{13}C$ and 0.13‰ for $\delta^{15}N$. Stable carbon isotope data from tusk dentin and hair are converted to $\delta^{13}C$ values of diet using enrichment factors, $\varepsilon^*_{diet\text{-}apatite}$ of 14.1‰ and $\varepsilon^*_{diet\text{-}hair}$ of 3.1‰ and converted to percent %C4 in diet using $\delta^{13}C$ values of a large data set of local plants to define C_3 and C_4 end members (Supplementary Information). For hair data, the dietary reconstruction is further modeled using the reaction progress variable (RPV) developed by Cerling et al. (2007). The RPV model attempts to reconstruct instantaneous $\delta^{13}C$ of diet from measured $\delta^{13}C$ values in hair by modeling tissue turnover as a series reactive pools that each have first order rate constants (Supplementary Information; Cerling et al., 2007).

3.4. Tusk and tail hair growth rates

The growth rate of serially sampled tissues must be known or determined in order to compare the stable isotope data to remote sensing and meteorological time series data. We use three methods to determine growth rates of tail hair and tusks. Full descriptions of how these methods were applied to the samples in this study are provided in the Supplementary Information. Tusk growth rates are expressed in microns per day (μm/day) in the radial direction, approximately normal to the axis of the tusk. Measurements were made on thin sections from transversely cut pieces of the tusk (Fig. 4) and the orientation of a tusk thin section is shown in Fig. 2. Hair growth rates are in millimeters per day (mm/day).

We use two methods to independently determine tusk growth rates, bomb-curve ^{14}C dating and histological methods (Supplementary Information). The histological method relies on counting growth increments with a known periodicity (e.g., Fisher, 1996, 2008; Fisher and Fox, 2003), which is seven days for African elephants. We measure the thickness of the weekly second-order growth increments on thin sections of the three tusk dentin slabs (Fig. 4). Measurements are made in the radial direction from the tusk axis toward the CDJ, which chronologically goes from more recent dentin at the axis to older dentin at the CDJ. Increment thicknesses are measured using an ImageJ plug-in called IncMeas (v1.2), then smoothed with a 10-point running mean (Rountrey, 2009). Finally, we tune stable isotope data based first on the calculated growth rates and then by the known relationship between $\delta^{13}C$ and NDVI (Cerling et al., 2009). To do the latter step, we align the $\delta^{13}C$ and NDVI peaks between two match points using the software program AnalySeries (v 2.0.4.2). After tuning, we shift each isotopic time series by +16 days to account for the lag between $\delta^{13}C$ and NDVI peaks (Cerling et al., 2009).

We determine growth rates from temporally overlapping tusk slabs and tail hairs by visual matching (VM) of their isotope profiles (Wittemyer et al., 2009). Visual matching enables overlapping time-series from tusk and hair samples to be combined into composite time series. Two of three tusk samples, slabs 1169 and 1053, are combined into a composite record that continues up to the death of R37, a known date. The other dentin slab, 412, has a single anchor-point age of 1985.54 (± 0.63 yr) that was determined through precise bomb curve ^{14}C dating (Uno et al., 2013). This part of the tusk would have formed when R37 was ~32 years old. The five tail hairs are also combined where possible but have a gap during a period where no hair was collected.

3.5. Data analyses and prediction

3.5.1. Time series analysis

Stable isotope data are analyzed for temporal correlations with NDVI and rainfall data. All time series data are interpolated using a spline function and then evenly resampled at a seven-day interval

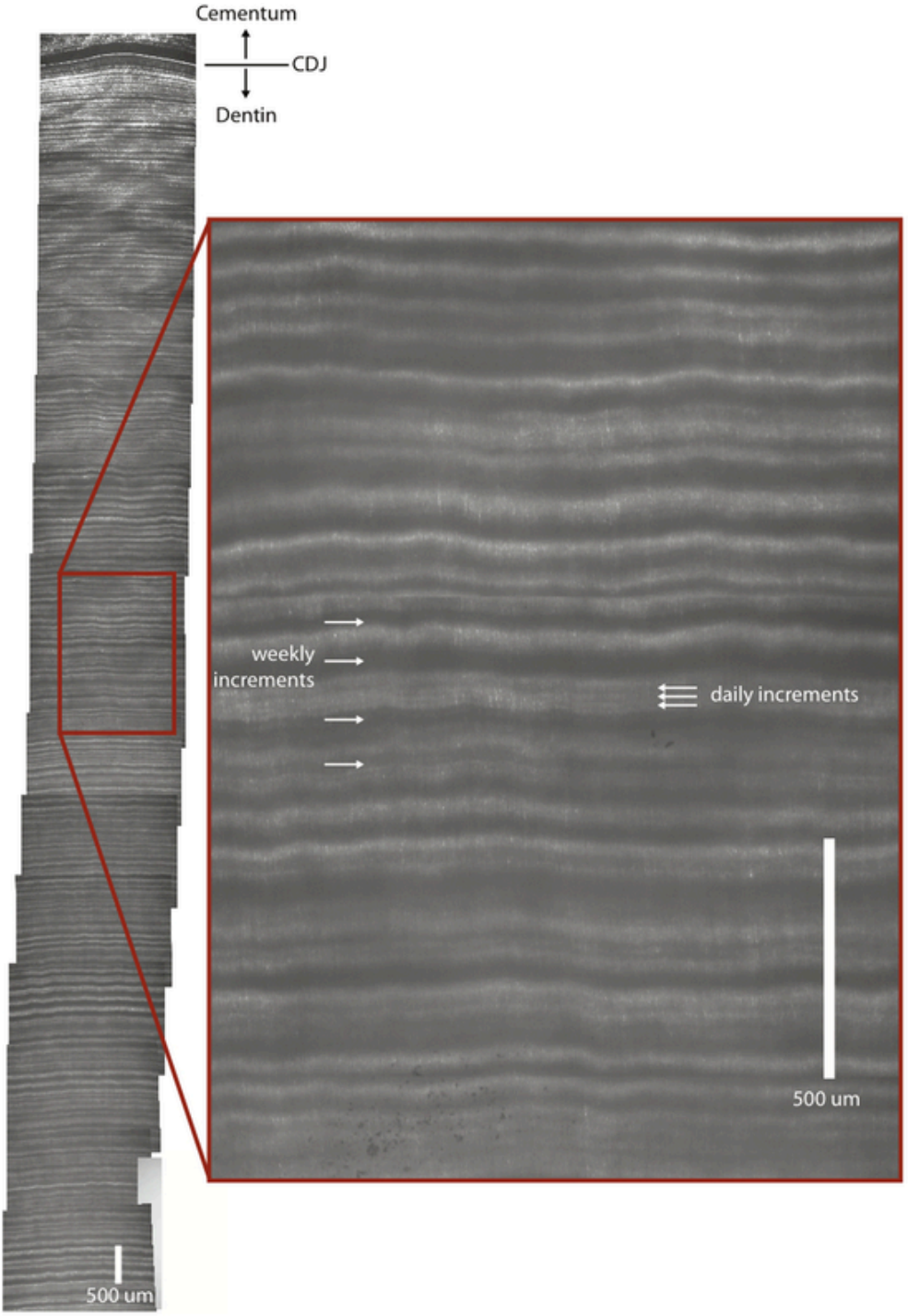

Fig. 4. Left: Mosaic of stitched photomicrographs from a thin section of sample 1169 at 35x magnification under transmitted plane-polarized light. Right: inset of composite thin section. Approximately weekly (second-order) and daily (third-order) increments are shown with arrows.

to match the resolution of the tusk dentin and hair samples. Following interpolation, we apply a 3 pt. convolution filter (0.25, 0.5, 0.25) to smooth the data. We assess time lags between rainfall, NDVI, and isotope signals through a series of linear regressions at different time lags (e.g., 0, 7, 14, and 21 days).

3.5.2. Least squares inverse filter

If the vegetation parameter NDVI and the dietary proxy $\delta^{13}C$ are denoted as two linearly related signals $x(t)$ and $y(t)$, respectively, a transfer filter $f(t)$ can be applied to predict $y(t)$ (i.e. $\delta^{13}C$) from $x(t)$ (i.e. NDVI):

$$y(t) = \int f(t-\tau)\, x(t)\, d\tau \tag{2}$$

where we assume temporal invariance in the transfer function so the above equation is that of convolution. The discrete form of this convolutional equation is given by

$$\mathbf{y=Xf} \tag{3}$$

where f is the Nx1 filter vector, X is the MxN convolution matrix for input NDVI data *x(t)* and y is the Mx1 output vector of isotope data *y(t)*. The optimal filter is the one that minimizes the sum of the squared residuals

$$\varepsilon = \tfrac{1}{2}\mathbf{r}^T\mathbf{r} = \tfrac{1}{2}(\mathbf{Xf}-\mathbf{y})^T(\mathbf{Xf}-\mathbf{y}) \quad (4)$$

so that the discrete least squares inverse filter is given as

$$\mathbf{f} = (\mathbf{XTX})^{-1}\mathbf{X}^T\mathbf{y} \quad (5)$$

In our case we use a causal filter *f(t)* where components are zero for $t < 0$. A small amount of damping is added to the diagonal component of X^TX to regularize the solution (Menke, 1989). Potential applications of the filter in Eq. (5) include using isotope profiles to reconstruct seasonality of vegetation in the past with Eq. (3) or, given the time history of NDVI, predict the diet of elephants from g in Eqs. (6) and (7).

The workflow for determining **f** (or **g**) and applying it to the data is the following.

1. *Training*. The goal is to find the optimal estimate of the transfer function f from the training pairs of data (x,y) and then use **f** in Eq. (3) to predict NVDI data $\mathbf{x}_{new}$ from $\mathbf{y}_{new}$. The training data will also be referred to as 'tuning' data because it is trained over a short interval of time that contains relevant pairs of known (**x**,**y**) data. These tuning data will be discretized into Mx1 vectors **x** and **y**, respectively, and the optimal filter is computed from Eq. (5). The NDVI data and the tuned $\delta^{13}C$ data are discretized at 10-day intervals, smoothed through convolution with a center-weighted three-point mean, demeaned, and normalized. A tuning interval of 600 days is used because it covers *ca.* three wet seasons. This is about one-third of the time represented in the 1982 to 1987 profile in which **f** is used to predict NDVI from $\delta^{13}C$.

We can also construct a set of equations that represents a transfer function **g** relating the NVDI data **x** to the isotope data **y**:

$$\mathbf{Yg}=\mathbf{x} \quad (6)$$

where **Y** is the convolution matrix for the isotope data. In this case, the least squares inverse filter **g** is given by

$$\mathbf{g} = \left(\mathbf{Y}^T\mathbf{Y}\right)^{-1}\mathbf{Y}^T\mathbf{x} \quad (7)$$

2. *Inference*. Once the filter **f** is constructed from Eq. (5) then, according to Eq. (3), it is applied to new isotope data **y** not seen in the training set to get the predictions **x** of the NDVI records from the new isotope data. The other transfer filter **g** from Eq. (7) can be used in Eq. (6) to predict isotope data **y** from NDVI data **x**.

4. Results

4.1. Tissue growth rates

4.1.1. Tusk growth rates

The growth rates determined by visual matching (VM) of $\delta^{13}C$ peaks with NDVI peaks range from 13.4 to 15.2 μm/day (Table 1). Growth rates from increment thickness measurements range from 12.8 to 15.4 μm/day. Measurements of the weekly, second-order growth increments from thin sections (n = 816) are available in Table S1 and shown for the three tusk dentin slabs in Fig. 5. A single ^{14}C-based growth rate from sample slab 1053 is 14.9 ± 0.6 (1σ) μm/day, which is nearly identical to the rate determined from the other two methods (Table 1). Tuned growth rates range from 13.3 to 14.6 μm/day, and using these, the time represented in each micromilled sample (100 μm width) is approximately weekly (6.8 to 7.1 days/sample). Based on the growth rates, the isotope profiles from sample 412 represent the period from June 1982 to April 1987 (4.81 years). The composite carbon and oxygen isotope profiles from samples 1053 and 1169 span the period from February 2000 to September 2006 (6.59 years).

Overall, tuning did not change the 2000 profiles very much. It had a moderate effect on the 412 profiles (Fig. S1). Untuned and tuned profiles for all samples are shown in Fig. S1 and S1A shows an overlapping period of 0.7 years between $\delta^{13}C$ profiles from 1169 and 1053 that were used to develop the composite record. The profiles from the 412 sample and the composite profiles from 1053 and 1169 samples are referred to as the 1982 and the 2000 profiles, respectively, from here onward.

4.1.2. Tail hair growth rates

Tuned growth rates from VM five R37 tail hairs have a mean value of 0.60 ± 0.03 mm/day and range from 0.55 to 0.62 mm/day (Table 2). Isotope profiles from each hair were combined using VM to make a composite hair record, which was then tuned to NDVI. Tuned growth rates vary little from the VM growth rates (Table 2). The average sampling interval is 8.3 ± 0.5 days, and the time represented in an individual hair ranges from 379 to 533 days. Based on the growth rates, the combined isotope profiles span a 6.9-year period from November 4, 1999 to September 26, 2006. There is a 2.2-year gap in the record from November 22, 2002 to February 5, 2005 due to a lack of sampling from November 2002 to June 2006. The date of the latter end of the gap, February 5, 2005, represents the distal end of the hair collected on June 17, 2006.

Table 1
Growth rates, sample thickness, and time represented in sampled intervals of tusk dentin slabs.

Sample ID	No. of samples	Sample width avg. ± 1σ (μm)	Dist. milled (μm)	Radial growth rate (um/day)				Days/sample avg ± 1σ [b]	Time in milled dentin slab (yrs.) [b]
				VM	INC [a]	^{14}C	Tuned		
R37-DEN-412	249	102 ± 24	25,400	14.0	15.4 ± 4.7	–	14.3	7.1 ± 1.7	4.8
R37-DEN-1053	225	100 ± 23	22,470	15.2	14.7 ± 4.1	14.9 ± 0.6	14.6	6.9 ± 1.6	4.2
R37-DEN-1169	150	91 ± 12	14,457	13.4	12.8 ± 3.6	–	13.3	6.8 ± 0.9	3.0

Note: VM and INC are visual matching and 2nd-order growth increments. VM and ^{14}C growth rates are linear.
[a] INC growth rate was calculated only from increments in the sampled interval. Growth rate data for the entire slab is shown in Fig. 5.
[b] Calculated from tuned growth rates.

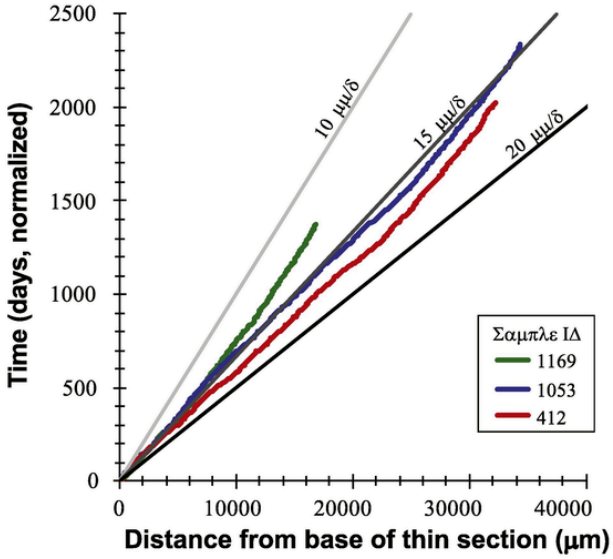

Fig. 5. Tusk growth rates calculated from second-order growth increment thicknesses for three tusk dentin slabs. Three modeled linear growth rates (10, 15, and 20 μm/day) are plotted as a reference. The base of each thin section is at or near the pulp cavity or tusk axis.

4.2. Stable isotope profiles

4.2.1. Stable isotope profiles in tusk dentin

The tuned tusk dentin $\delta^{13}C$ and $\delta^{18}O$ ($\delta^{13}C_{dentin}$ and $\delta^{18}O_{dentin}$, respectively) data (n = 239) from the 1982 profiles span 5.8 years. Data from the combined 1169 (n = 143; 2.9 years) and 1053 (n = 215; 4.2 years) profiles form the 2000 profiles (n = 331) that span 6.6 years. Table 3 contains descriptive statistics for isotope data from the profiles, and all tusk dentin isotope data are provided in Table S2. The 1982 profiles are plotted in , along with rainfall and NDVI data (Tables S3 and S4) and the 2000 profiles are plotted in Fig. 7. The mean $\delta^{13}C$ and $\delta^{18}O$ values from the 1982 profiles are −11.8 ± 0.9 (1σ) and −4.7 ± 0.8‰. Values for the 2000 profiles are similar, −11.2 ± 0.8 and −3.9 ± 0.9‰, respectively. Diet ranges from 5 to 35%C4 (mean 14.5%C4) in the 1982 profile and from 7 to 39%C4 (mean 18.5%C4) in the 2000 profile. We explore relationships between rainfall, NDVI, $\delta^{13}C_{diet}$, and $\delta^{18}O_{dentin}$ series through a series of linear regressions with different time lags (e.g., 0, 7, 14 days). The regressions show the highest correlations are between rainfall and NDVI and between NDVI and $\delta^{13}C_{diet}$ (Figs. 2–S7). The highest coefficients of determination (R^2 = 0.20 to 0.23) suggest NDVI maxima occur 14–21 days after rainfall maxima (Table S5). The $\delta^{13}C$ maxima occur 14 to 21 days after NDVI maxima (R^2 = 0.20 to 0.38), but regressions were performed on tuned data, where $\delta^{13}C$ and NDVI maxima were used as tie points and then $\delta^{13}C$ maxima were lagged 16 days, so a correlation is expected.

4.2.2. Stable isotope profiles in tail hair

The $\delta^{13}C$ and $\delta^{15}N$ values from five tail hairs (n = 272) were combined into composite profiles (n = 203; Fig. 8). All hair isotope data are given in Table S6. Tail hair $\delta^{13}C$ ($\delta^{13}C_{hair}$) has a mean value of −21.4 ± 0.9‰. Hair $\delta^{15}N$ ($\delta^{15}N_{hair}$) has a mean value of +11.0 ± 1.1‰. The $\delta^{13}C_{hair}$ and $\delta^{15}N_{hair}$ values covary throughout most of the record and are weakly correlated (R^2 = 0.102). Diet ranges from 9 to 46%C4 (mean: 21%C4) in the hair profile. The diet range increases from 0 to 68%C4 (mean 21%C4) when the RPV model is applied to the hair profile (Fig. 8C). The tuned $\delta^{13}C_{dentin}$ and $\delta^{13}C_{hair}$ profiles from 2000 to 2006, are converted to $\delta^{13}C_{diet}$, and plotted in Fig. 9. The profiles show remarkable agreement with residuals between the dentin and hair records less than ±1‰ for most of the record (Fig. 9B).

4.3. Least squares inverse filter

Least squares inverse filter results yield profiles of predicted $\delta^{13}C$ from NDVI (Fig. 10) and vice versa, predicted NDVI from $\delta^{13}C$ (Fig. 11) for the 1982 profile. Predicted and actual profiles for both variables show good agreement in locations of peak maxima and peak widths. A linear regression of predicted and actual $\delta^{13}C$ values indicates the least squares inverse filter performs relatively well, where $\delta^{13}C_{pred} = 0.64 \times \delta^{13}C_{actual} - 3.9$ (R^2 = 0.563). A linear regression for NDVI returns a lower slope and R^2 value: $NDVI_{pred} = 0.35 \times NDVI_{actual} + 0.166$ (R^2 = 0.344). Residuals of actual minus predicted values are <2‰ for $\delta^{13}C$ and generally <0.1 but up to 0.3 for NDVI (Figs. 10A and 11A).

5. Discussion

5.1. Tissue growth rates

The consilience in growth rates from the three different methods suggest each method can be applied on its own to future studies of proboscidean tusks. This comes with several caveats. First, the time represented in second-order growth increments can vary in different proboscidean taxa. It is weekly in L. *africana*, but fortnightly in the mastodon *Mammut americanum* (Fisher, 1987). Second, there can be variation in increment thickness resulting from position along the pulp cavity surface. This variation is minimal except at either end of the pulp cavity. Measurements should be avoided near the horn (e.g., the tusk axis) and near the margin. There, growth rates appear to decrease, resulting in thinner increments, as demonstrated by the gentle, concave-up geometry at the distal end of the growth curves in Fig. 5. A coeval period (2003 to 2006) from dentin slabs 1053 and 1169 shows that the latter piece, located closer to the pulp cavity margin, had a lower growth rate.

Table 2
Tail hair lengths and growth rates based on visual matching of isotope profiles.

Tail hair sample ID	Sample date	Length (mm)	Growth rate (mm/day)		Days/sample [a]	Time in hair [a]	
			VM	Tuned	Avg ± 1σ	Days	Years
R37-010125	25-Jan-01	310	0.69 ± 0.03	0.61 ± 0.03	8.2 ± 0.4	508	1.39
R37-020204	4-Feb-02	330	0.63 ± 0.03	0.60 ± 0.03	7.9 ± 0.4	524	1.43
R37-021101	1-Nov-02	235	0.59 ± 0.03	0.62 ± 0.03	8.1 ± 0.4	379	1.04
R37-060617	17-Jun-06	320	0.60 ± 0.03	0.60 ± 0.03	8.3 ± 0.4	533	1.46
R37-060627	27-Sep-06	290	0.55 ± 0.03	0.55 ± 0.03	9.1 ± 0.5	527	1.44

Note: VM is visual matching.
[a] Calculated from tuned growth rates.

Table 3
Descriptive statistics from tusk dentin and hair profiles.

Profile	(‰)				$\%C_4$ [d]
	$\delta^{13}C$ [a]	$\delta^{18}O$ [a]	$\delta^{15}N$ [b]	$\delta^{13}C_{diet}$ [c]	
Tusk dentin (412) min.	−13.1	−7.1	–	−26.7	5.0
(n = 239) max.	−8.9	−2.1	–	−22.5	35.1
Range	4.2	5.0	–	4.2	30.1
Avg.	−11.8	−4.7	–	−25.4	14.5
1σ	0.9	0.8	–	0.9	6.2
Tusk dentin (1169 & 1053) min.	−12.9	−6.6	–	−26.5	6.6
(n = 331) max.	−8.4	−1.2	–	−22.0	38.5
Range	4.5	5.4	–	4.5	32.0
Avg.	−11.2	−3.9	–	−24.8	18.5
1σ	0.8	0.9	–	0.8	6.0
Hair min.	−23.0	–	8.1	−26.1	9.6
(n = 203) max.	−17.9	–	14.2	−21.0	45.6
Range	5.0	–	6.1	5.0	36.0
Avg.	−21.4	–	11.0	−24.5	20.5
1σ	0.9	–	1.1	0.9	6.3
				$\delta^{13}C_{diet}$ [d,e]	**$\%C_4$ [d,e]**
Hair (RPV) min.	–	–	–	−27.4	0.0
(n = 203) max.	–	–	–	−17.9	67.7
Range	–	–	–	9.5	67.7
Avg.	–	–	–	−24.5	21.0
1σ	–	–	–	1.5	10.8

Note: a) vs.VPDB; b) vs. AIR; c) diet calculations based on $\varepsilon_{diet\text{-}apatite}$ and $\varepsilon_{diet\text{-}keratin}$ of +13.6 and +3.1, respectively; d) %C4 calculations based on end-member values for C3 and C4 plants given in Supplementary Information; e) diet calculated using the RPV model from Cerling et al. (2007).

Second-order increment thickness, which reflects tusk growth rate, is highly variable in the R37 tusk. It exhibits a quasi-periodic structure that may contain life history and climate information. Periods of higher growth rate appear to correspond to rainy seasons and periods of higher NPP (Fig. S8). Using second-order increment thicknesses, Fisher and colleagues have shown that tusk growth rates in extinct proboscideans decrease during winters in temperate regions (Fisher et al., 2003; Koch et al., 1989) and that tusk growth rates may also be affected by (~3–6 year) calving cycles in mastodons (Fisher, 1996; Fisher, 2008). Additional histological studies on African elephant tusks with known life histories, such as that of R37, could confirm whether calving events are preserved in tusks.

As for other incremental growth features, we note that while the second-order growth increments are prominent in R37's thin sections and polished slabs (Figs. 3 and 4), first-order (annual) increments observed in other proboscidean tusks are not clearly resolvable. This may be due to the lack of strong annual variability in temperature in tropical East Africa, which is likely the primary cause for annual incremental features. This does not mean first-order increments are lacking in all L. *africana* tusks. Codron et al. (2012) report first-order increments in seven tusks from South Africa, where annual seasonality is present, and they have been documented in other polished transverse sections of L. *africana* tusks (plate 32, Sikes, 1971).

5.2. Stable isotope profiles

5.2.1. Stable isotopes in tusk dentin

The most striking feature of the isotope data is the close relationship between rainfall, NDVI, and $\delta^{13}C_{dentin}$ that rise and fall, nearly in concert (Figs. 6 and 7). The data demonstrate that $\delta^{13}C_{dentin}$ values serve as a proxies for seasonal changes in diet, vegetation, and rainfall.

5.2.1.1. Carbon isotopes in tusk dentin As megaherbivores, elephants are dietary generalists, and the carbon isotope profiles illustrate how they opportunistically feed on C_4 vegetation during and just after the wet season. The C_4 vegetation in their diet is predominantly grasses (Supplementary Information), so this represents a fundamental shift in their feeding habit from browsing to mixed feeding (Figs. 6 and 7). The highly variable diet and plasticity in their feeding habit represents an advantage over dietary specialists during times of limited resource availably due to droughts or ecosystem disturbance (fire, locusts, etc.). There are several possible reasons for the dietary switch to C_4 grasses during the wet season, all of which are advantageous for elephants. One is that the grasses become widely available and therefore require less foraging movement, making it metabolically more efficient. Another is that the grasses, especially when still wet, are more digestible than the typical diet of woody vegetation. A third reason, proposed by Cerling et al. (2009), is that elephants seek out grasses because of their higher crude protein content compared to woody vegetation.The increased consumption of C_4 grasses following increases in NDVI is not linear, although each NDVI peak in the profiles is associated with an increase in $\delta^{13}C_{dentin}$ (Figs. 6 and 7). Large NDVI peaks values do not always result in large $\delta^{13}C_{dentin}$ peaks. The highest NDVI peak (>0.6 max.) in the 1982 profile occurs in the fall of 1982 during the short rains, followed by a relatively small peak (0.42 max.) during the long rains of 1983 (Fig. 6). Yet the $\delta^{13}C_{dentin}$ peak during the short rains of 1982 is smaller (in height and width) than the subsequent peak in 1983. The reason for the occasional lack of scaling between peak sizes in NDVI and $\delta^{13}C_{dentin}$ is that elephants' dietary choices involve nutritional considerations (e.g., in relation to reproductive state) and ecological drivers relating to resource access (e.g., socially driven (Wittemyer et al., 2007) or predation-related (Ihwagi et al., 2015)). Although the $\delta^{13}C_{dentin}$ to NDVI relationship does not always scale linearly, the data show that every NDVI peak in both profiles has a corresponding $\delta^{13}C_{dentin}$ peak (Figs. 6 and 7).

5.2.2. Oxygen isotopes in tusk dentin

The $\delta^{18}O_{dentin}$ profiles show an oscillatory pattern similar to the $\delta^{13}C_{dentin}$ profiles (and coincide approximately with NDVI peaks (Figs. 6 and 7). We interpret the pattern of increased $\delta^{18}O_{dentin}$ values as reflecting changes in R37's body water ($\delta^{18}O_{bw}$) caused by seasonal shifts in water intake. Kohn (1996) suggests that the primary source of oxygen in body water of wild, large herbivores, is plant water (ca. 50%), followed by water vapor in air (24%), drinking water (<20%), and water structurally bound in food (<10%). Thus, variation in the $\delta^{18}O$ of plant water and to a lesser extent, drinking water, control the $\delta^{18}O$ of body water ($\delta^{18}O_{bw}$), and ultimately $\delta^{18}O_{dentin}$. During the wet season, we propose there is an increase in the fraction of ^{18}O-enriched plant water and a decrease in the fraction of ^{18}O-depleted drinking water in the elephant's body water pool.

Elephants are obligate drinkers, and during the dry season especially, elephants in and around the Reserves drink daily from the Ewaso Ng'iro or one of its permanent tributaries. During the wet season, water availability away from permanent sources increases, including from plant water, as the elephants become less reliant on the Ewaso Ng'iro River, and their range expands to areas where C_4 grasses are more abundant (Wittemyer et al., 2007; Cerling et al., 2009). The GPS data for R37 from 2001 support this interpretation of shifting reliance from permanent water sources, such as the Ewaso Ng'iro River. From July 11 to December 31, 2001, R37 visited permanent water sources 83% of the days during the dry season but only 34% of the days during the wet season (Wittemyer et al., 2008).

The process leading to increased $\delta^{18}O_{dentin}$ values does not just occur during wet seasons though. The two highest $\delta^{18}O_{dentin}$ peaks in the 1982 profile come back to back during the extreme drought of 1983–1984 that led to widespread famine in East Africa, especially

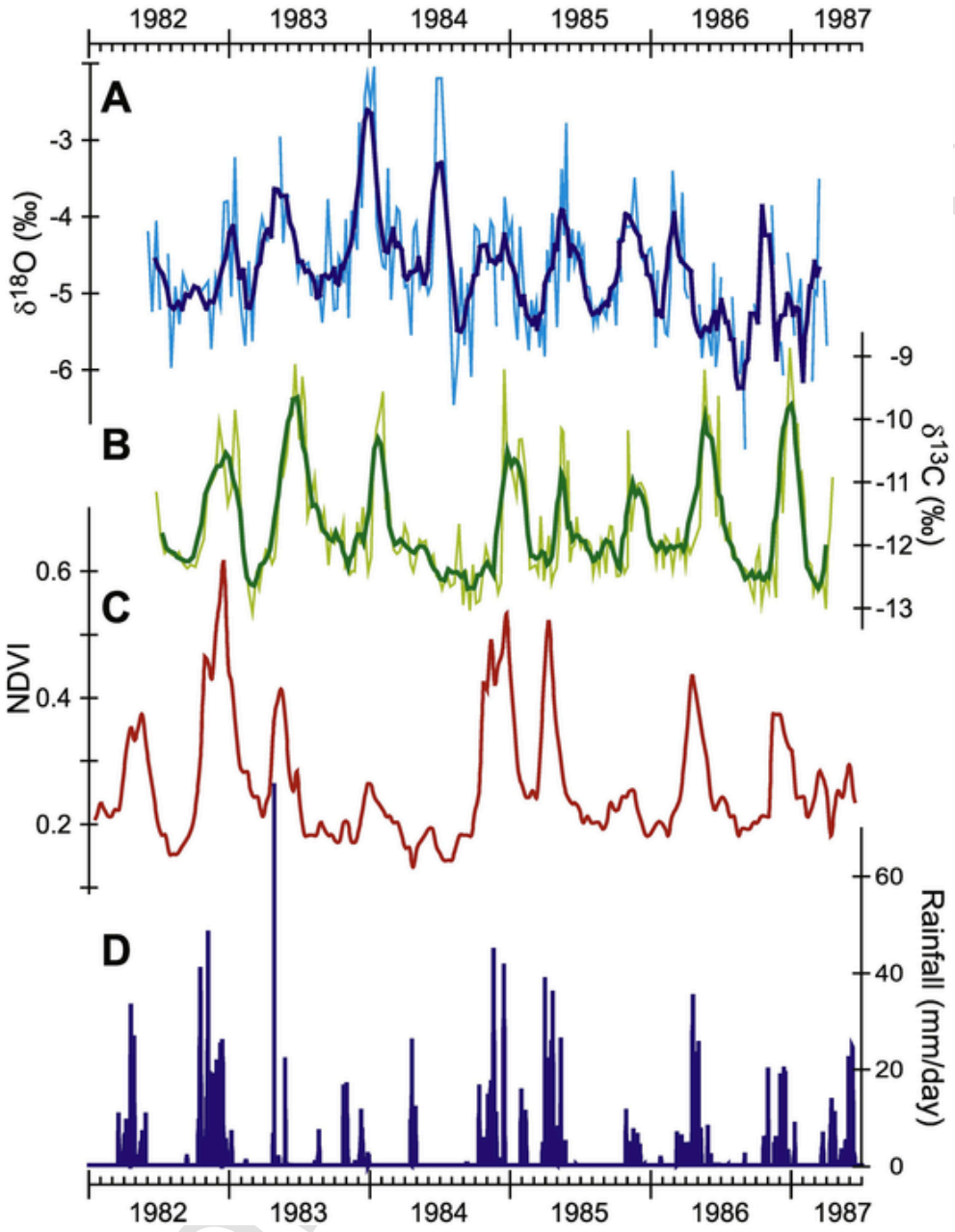

Fig. 6. Stacked rainfall, Normalized Difference Vegetation Index, $\delta^{13}C$, and $\delta^{18}O$ (both in VPDB) plots of tuned composite tusk dentin profiles from slab 412 for the interval of 1982 to 1987. Bold lines in the $\delta^{13}C$ and $\delta^{18}O$ profiles are 5-point running means. Rainfall data were collected at Archer's Post by the East African Meteorological Department.

in Ethiopia. The usual wet seasons and NDVI responses were subdued and there is no $\delta^{13}C_{dentin}$ peak associated with the long rains in 1984 (Fig. 6). What then causes the anomalously high $\delta^{18}O_{dentin}$ peaks? The most likely scenario is that even permanent water sources were significantly evaporated and all water sources, including rivers, water holes, and plant water, were enriched in ^{18}O relative to normal conditions.

Cerling et al. (2009) present δD tail hair (δD_{hair}) from the socially dominant family unit in the Reserves, the Royals, and δD water (δD_w) data from the Ewaso Ng'iro River and find the opposite trend in Royal's tail hair from what we observe in R37's $\delta^{18}O$ tusk profiles. Royal's δD_{hair} shows a strong positive correation with δD_w ($R^2 = 0.64$) such that during rainy seasons when δD_w of the Ewaso Ng'iro becomes more negative, δD_{hair} does, too (Fig. 5 in Cerling et al., 2009). The seasonal change in river water, ranging from −28 to +11‰ in δD (~ −5 to 0‰ in $\delta^{18}O$) is caused by evaporative enrichment of ^{18}O and D in the river during the dry season. The evaporative enrichment is more pronounced in plants due to the compounding evaporation processes of soil water and leaf water. As the dominant group in the Reserves, the Royals continue to utilize the Ewaso Ng'iro during the wet season, visiting the river on 84% of the days between July to December 2001 (Wittemyer et al., 2008). GPS data allow us to determine that differences in water intake are most likely the cause for the opposite trends observed in R37's $\delta^{18}O_{dentin}$ and the δD_{hair} from the Royals, and may even be interpreted as rank-driven resource partitioning. The combination of meteorological, observational, and remote sensing data used here to interpret body water isotope records highlights the complexity and equifinality in interpretation and suggests caution in studies where these auxiliary data are not available.

5.2.3. Stable isotopes in tail hair

Overall $\delta^{13}C_{hair}$ and $\delta^{15}N_{hair}$ in the composite profile covary (Fig. 8), but there are several periods in the hair profile that deserve fo-

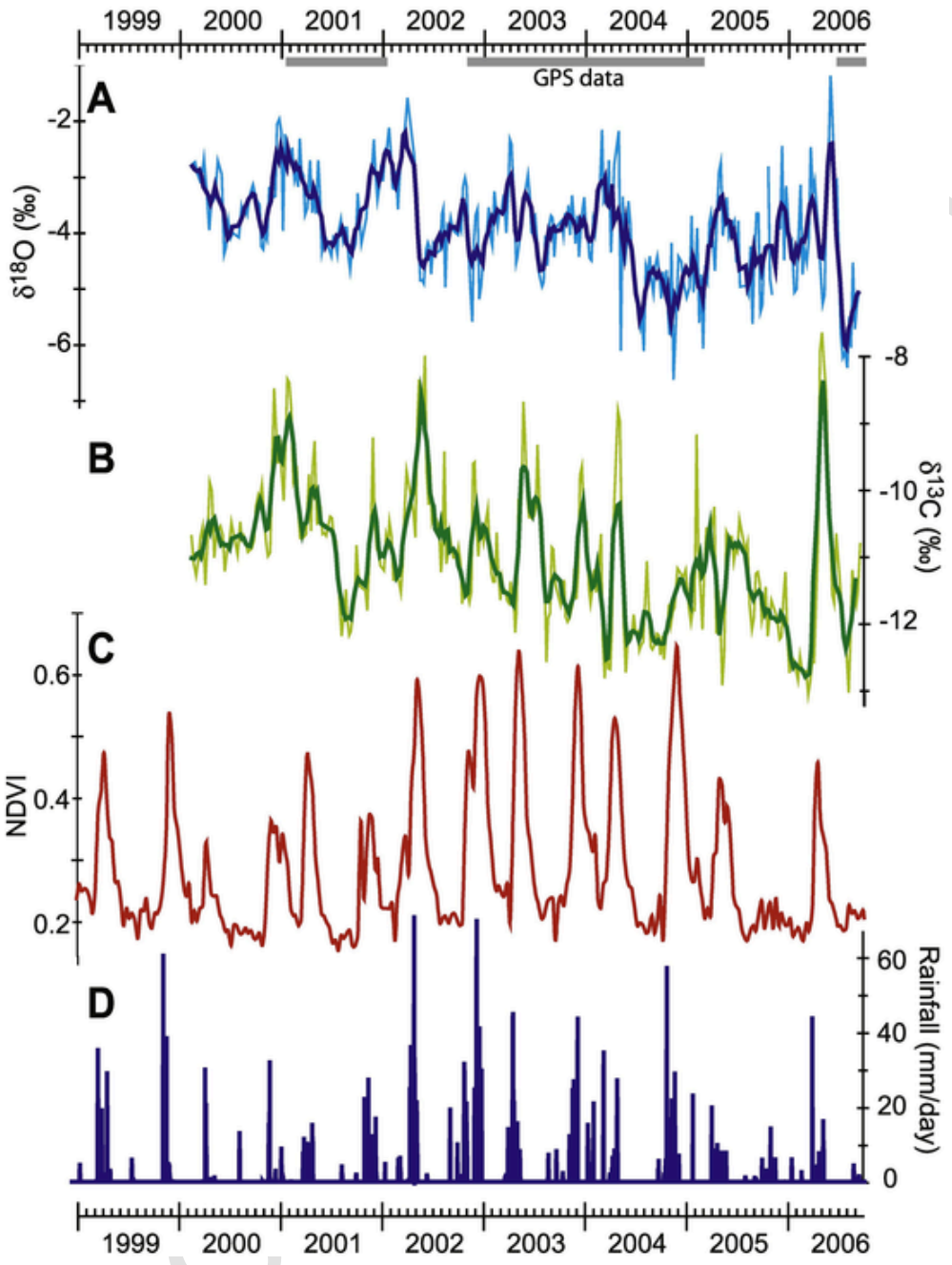

Fig. 7. Stacked rainfall, NDVI, $\delta^{13}C$, and δ^{18}(both in VPDB) O plots of tuned composite tusk dentin profiles from slabs 1169 and 1053 for the interval of 1999 to 2006. Bold lines in the $\delta^{13}C$ and $\delta^{18}O$ profiles are 5-point running means. Rainfall data were collected at Archer's Post by the East African Meteorological Department.

cus. The first is a period of anomalously low $\delta^{15}N_{hair}$ values (~2σ deviation from the mean) from December 2005 through mid-March 2006, when the short rains fail and the usual NDVI increase is absent. In the hair profile, this is preceded by the largest decrease in the $\delta^{15}N_{hair}$ profile from +12‰ to the lowest recorded values (<9‰) beginning in September 2005. The $\delta^{13}C_{hair}$ values also decrease and remain low during this period; it represents the longest interval of low $\%C_4$ in diet (10 to 15%) in the hair profile (Fig. 8). The $\delta^{15}N_{hair}$ data further suggest that all or some of the dietary resources during this period had relatively low $\delta^{15}N_{plant}$ values. Given that the trophic level enrichment is about +1 to +3‰ for $\delta^{15}N$, and the available isotopic data from plants, the diet during this period likely included *Indigofera schimperi,* an arid-adapted nitrogen fixing plant that is commonly consumed by elephants in the Reserves based on feeding observations (see Supplementary Information for discussion of plant isotopes). The values remain low until arrival of the long rains in 2006, when both increase rapidly as C_4 vegetation becomes a significant dietary component (>25%) for the first time in nearly 9 months.

A second noteworthy trend is the large-scale decoupling of the positive relationship between $\delta^{13}C_{hair}$ and $\delta^{15}N_{hair}$. This occurs twice in the hair profile, once in the middle of 2002 (May to August) and again from mid-June 2006 until death in September 2006. In the 2002 event, the $\delta^{13}C_{hair}$ decreases from −19 to −23‰ following the end of the long rains, which corresponds to a drop from 50 to ~0% C_4 vegetation in diet, followed by a rebound to ~15–20% C_4 (Fig. 8). During this period, the $\delta^{15}N_{hair}$ remains constant (~ +12‰) when the $\delta^{13}C_{hair}$ decreases, and then increases by one permil as $\delta^{13}C_{hair}$ stabilizes. Decoupling of $\delta^{13}C_{hair}$ and $\delta^{15}N_{hair}$ occurs again at the end of May

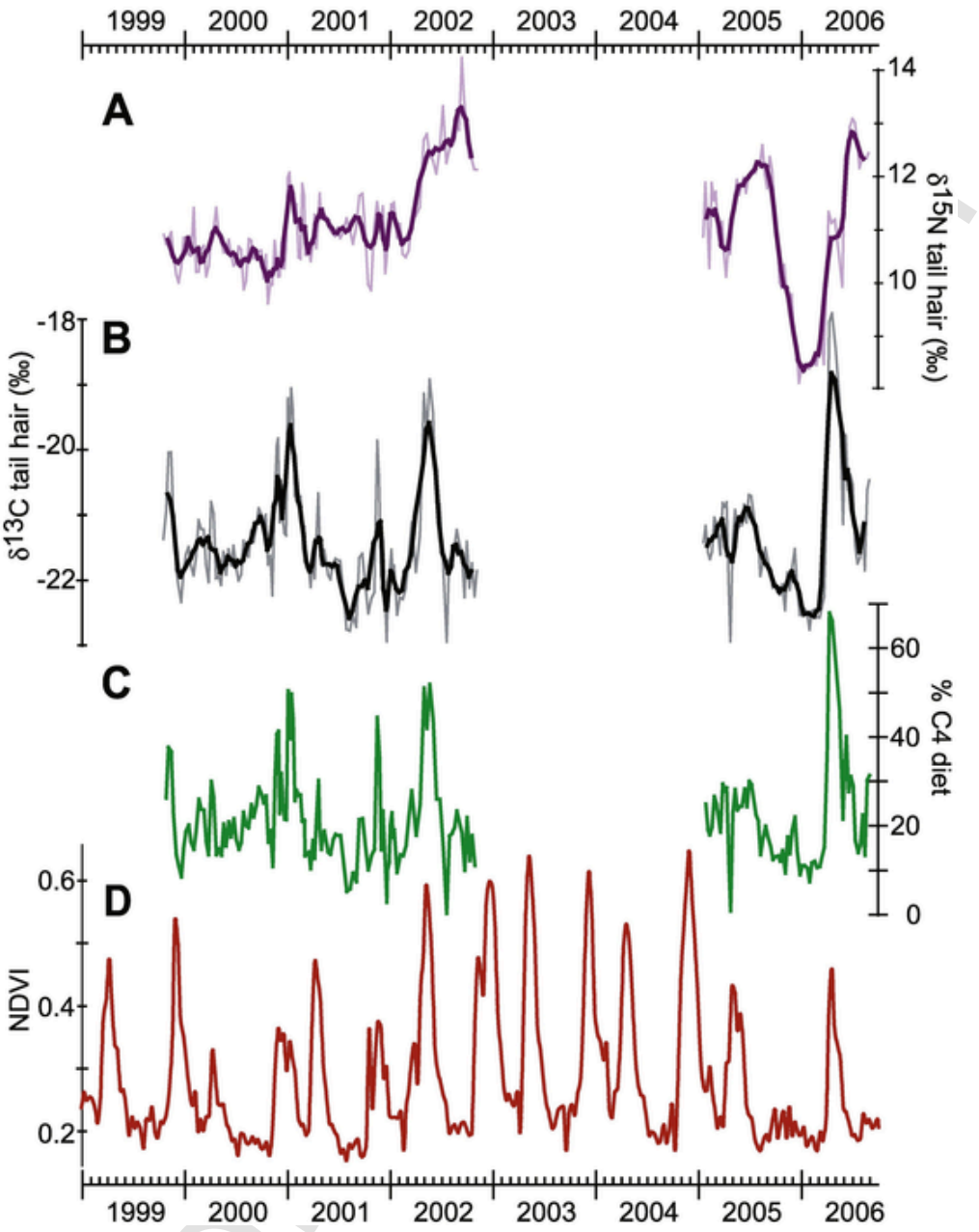

Fig. 8. Tail hair isotope and diet profiles for the interval of 1999 to 2006. A) and B) are $\delta^{15}N$ (AIR) and $\delta^{13}C$ (VPDB) values of tuned composite tail hair profiles, respectively. Bold lines in A) and B) are 5-point running means. C) Calculated $\%C_4$ in diet using the Reaction Progress Variable model (Cerling et al., 2007); D) Normalized Difference Vegetation Index.

2006, when $\delta^{13}C_{hair}$ is decreasing following the end of the long rains and $\delta^{15}N_{hair}$ increases from +10 to +13‰ by mid-July 2006. The decoupling of the $\delta^{13}C_{hair}$ and $\delta^{15}N_{hair}$ is either a result of diet, physiological processes, or a combination of the two. Even with the plant isotope data, it is difficult to determine which of these possibilities might be the more important factor.

5.2.4. Comparison of $\delta^{13}C$ profiles from tail hair and tusk dentin

Tail hair and tusk dentin $\delta^{13}C$ profiles from 2000 to 2006 are the first, to our knowledge, high-resolution hair and dentin records to be directly compared. Profile data from each tissue were converted to $\delta^{13}C_{diet}$, interpolated, and resampled at weekly intervals (Fig. 9A). There is remarkable agreement between the two profiles in range (Table 3) and high-frequency variability from week to week (Fig. 9A), despite periods of offset of >1‰ as shown by the residuals (Fig. 9B). Examination of the profile residuals reveals that between 2000 and 2002, $\delta^{13}C_{diet}$ from dentin ($\delta^{13}C_{diet\_dentin}$) is on average 0.5‰ more positive than $\delta^{13}C_{diet}$ from hair ($\delta^{13}C_{diet\_hair}$), and from 2005 through 2006, it is 0.4‰ more negative with respect to $\delta^{13}C_{diet\_hair}$. An important question to consider is: "What drives decoupling of $\delta^{13}C$ between the profiles?" The carbon isotope ratios in hair and tusk bioapatite both ultimately derive from diet, but differences in formation and composition of the tissues result in slight variation between the calculated $\delta^{13}C_{diet}$ from each tissue. We limit the discussion here to considerations of possible reasons for this primary observation, but provide an extended discussion in the Supplementary Information section, *Carbon Isotopes in hair and tusk dentin*.

Carbon in hair and dentin is incorporated through different metabolic pathways and sources, although ultimately it comes from food. Hair is made up of keratin, which consists mostly of proteins derived from amino acids. Amino acids used to construct hair are pulled from the blood stream at the follicle. The pool of available amino acids

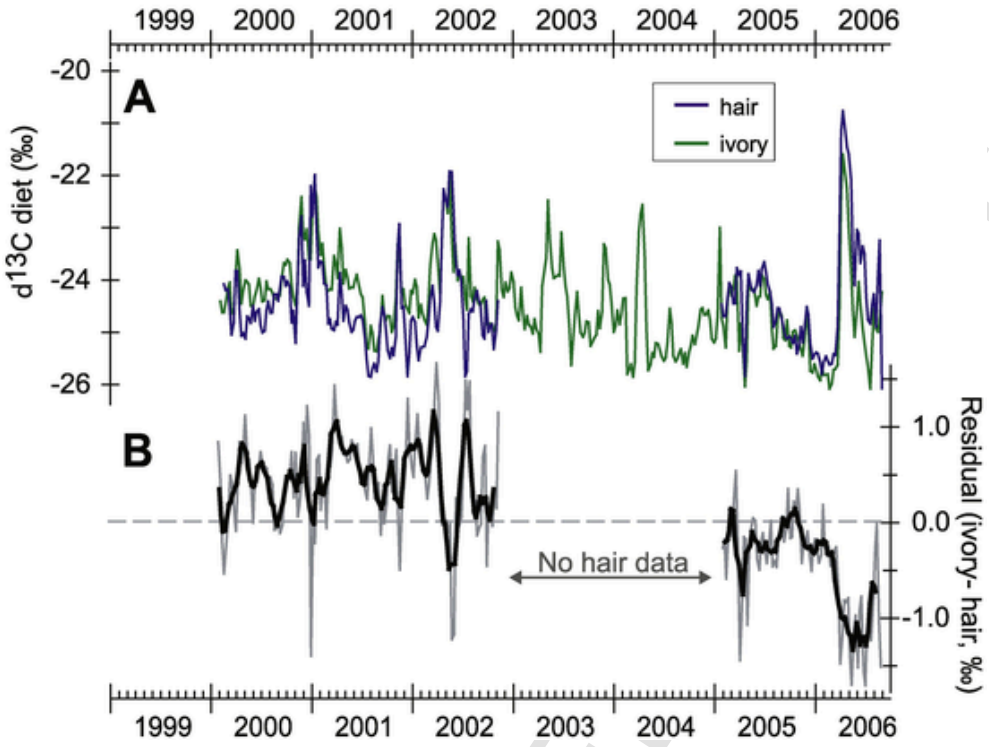

Fig. 9. A) The $\delta^{13}C_{diet}$ (VPDB) calculated from tusk dentin (green line) and hair (blue line) using enrichment factors of +14.1‰ and +3.1‰ for diet-apatite and diet-keratin, respectively. B) Residual plot of $\delta^{13}C_{diet(dentin)}$–$\delta^{13}C_{diet\ (hair)}$. Bold line is 5-point running mean. (For interpretation of the references to colour in this figure legend, the reader is referred to the web version of this article.)

in the blood stream can come from an exogenous source (i.e., diet), or they can come from endogenous sources via the breakdown of existing proteins in tissues (e.g., muscle, organ, etc.) or bone collagen (e.g., Ayliffe et al., 2004 and references therein). Endogenous sources have different concentrations of hair-forming amino acids and they also have different turnover rates, which are principally a function of metabolic activity. Ayliffe et al. (2004) determined that in horse tail hair, ~56% of the carbon isotope ratio in hair is determined by current diet (e.g., in the past five days), whereas 44% comes from diet over the past ~150 days, which is stored in tissues and skeletal material.

Carbon in the bioapatite of tusk dentin on the other hand, is derived from blood bicarbonate, which is the dominant carbonate species in the blood dissolved inorganic carbon (DIC) pool. Blood bicarbonate comes from cell-respired CO_2 produced through catabolism of carbohydrates and to a lesser extent, lipids and available proteins. Previous studies on the $\delta^{13}C$ of bioapatite and CO_2 of breath suggest a constant enrichment between breath and bioapatite ($\varepsilon^*_{breath\text{-}apatite}$) of ~ +11‰ (Passey et al., 2005; Tieszen and Fagre, 1993). In the same study on horse tail hair by Ayliffe et al. (2004), the authors found that 84% of the carbon isotope ratio in blood bicarbonate is determined by current diet (e.g., in the past 3 days), whereas only 16% comes from diet over the past ~50 days, which is stored in tissues and skeletal material. These metabolic sources and turnover rates suggest carbon isotopes in dentin should respond to diet shifts faster than hair and therefore record greater increases in the $\delta^{13}C$. The data suggest otherwise; there is slightly greater range in the $\delta^{13}C_{hair}$ profile than in the $\delta^{13}C_{dentin}$ profile (Fig. 9 and Table 3).

The difference between $\delta^{13}C_{diet}$ profiles is amplified when the RPV model is applied to the $\delta^{13}C_{hair}$ data, which takes into account long-term tissue turnover to reconstruct instantaneous diet. The RPV model results in a much higher range of diet (0 to 68%C4 in diet, Fig. 8C) than does the dentin profile data (7 to 39%C4, Table 3). The potential factors that could lead to the lower amplitudes measured in the $\delta^{13}C_{dentin}$ profile—dentin mineralization processes, temporal mixing from microdrilling of dentin, analytical challenges of acid hydrolysis of tusk dentin, or carbon routing of plant macronutrients (protein vs. carbohydrates) to hair vs. dentin—are discussed in detail in the Supplementary Information. The comparison of $\delta^{13}C$ profiles in dentin, hair, and RPV-modeled diet bring to light for the first time challenges in interpreting high-resolution isotopic data and highlight opportunities for additional study of tissue turnover and sampling methods to understand the offsets in reconstructed diet.

5.3. Least squares inverse filter predictions of diet and NDVI

The least squares inverse filter accurately predicts the frequency of seasonal changes using one environmental signal to predict the other. Differences in peak heights between predicted and actual peak height for both $\delta^{13}C$ and NDVI profiles seem to preclude the use of this technique for quantitatively evaluating the magnitude of seasonal change in vegetation or by proxy, rainfall, until further improvements can be made. Predicted carbon peaks match the frequency of actual peaks, but the baseline $\delta^{13}C$ value is ~0.5‰ higher than the actual value, and maximum peak values differ by up to 1.5‰ (Fig. 10B), which translates to a difference of 11%C_4. Predicted NDVI profiles also maintain the same peak frequency as their actual counterparts, but there are differences in peak shape and height, and a slight positive shift in location of peaks for predicted NDVI (Fig. 11).

5.4. Applications of tusk isotope profiles to modern ecology and paleoecology

The results of this study have implications for modern ecology and terrestrial paleoecology. In C_3–C_4 ecosystems where tail hair or tusks can be collected, isotope profiles reveal seasonal variations in vegetation, precipitation, and individual diet. For hair, these methods have been applied to numerous studies of marine and terrestrial mammals (e.g., Cerling et al., 2009; Codron et al., 2013; Darimont

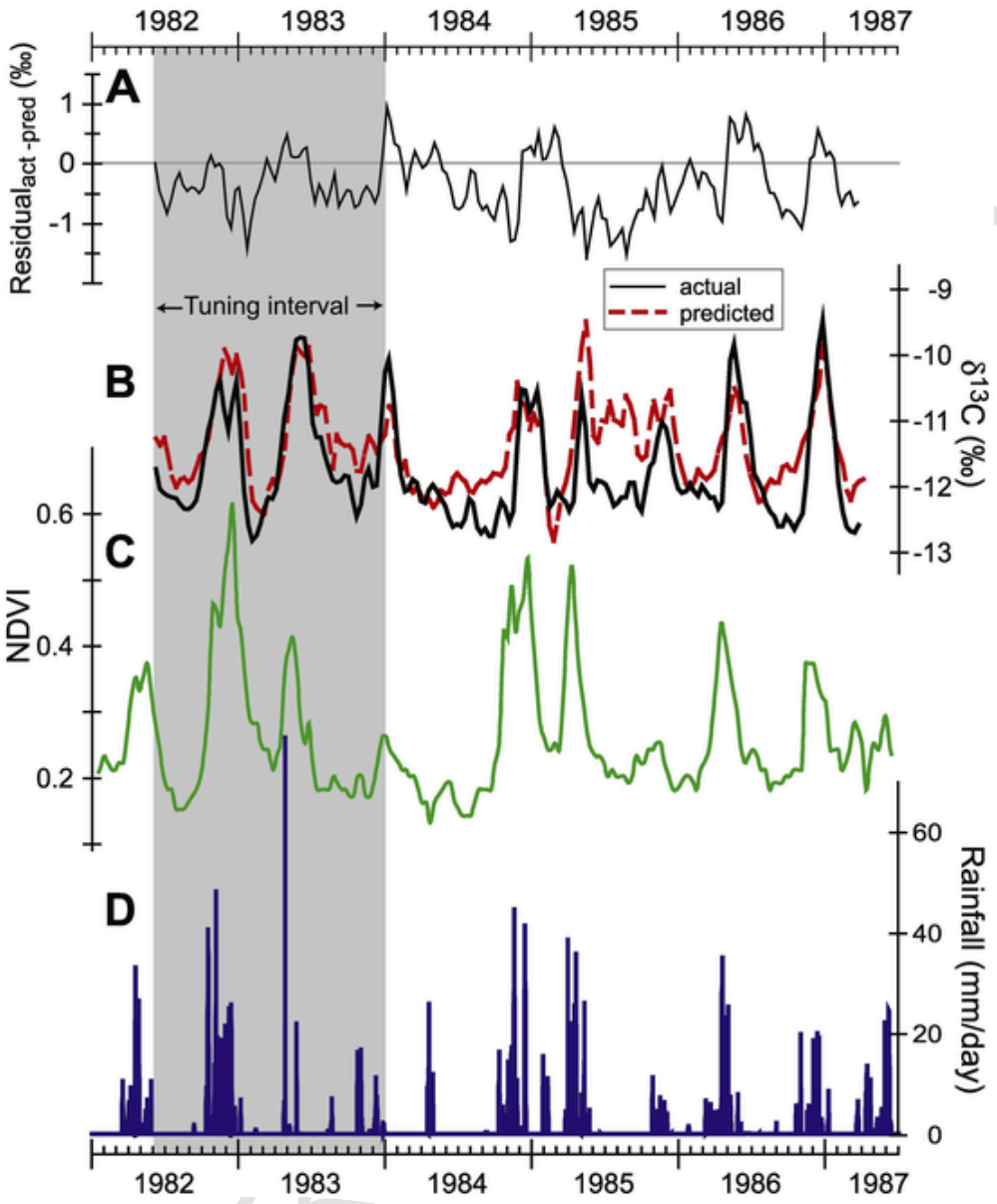

Fig. 10. Matching filter results for predicted $\delta^{13}C$ (VPDB) based on Normalized Difference Vegetation Index data compared to actual $\delta^{13}C_{dentin}$ data from 1982 to 1987. A) Residual between actual and predicted $\delta^{13}C$, B) actual (black) vs. predicted (red dashed) $\delta^{13}C$, C) NDVI that served as matching filter input, and D) rainfall. The shaded box represents the 600-day tuning interval. Rainfall data were collected at Archer's Post by the East African Meteorological Department. (For interpretation of the references to colour in this figure legend, the reader is referred to the web version of this article.)

and Reimchen, 2002; Newsome et al., 2009). From a practical standpoint, stable isotope profiles are an efficient and less resource intensive alternative for studying diet than traditional methods such as feces collection and feeding observations. Potential applications to modern ecology and social behavior could include comparing multiyear isotope profiles from elephants of different social rank within a population to understand how hierarchal position affects access to resources during the dry season, when more limited access to available water sources and forage generates competition among family units (Wittemyer and Getz, 2007).

Long-term tusk isotope profiles have the potential to elucidate changes in diet over multiyear periods. Long profiles can improve our understanding of the relationship between elephants, vegetation, and land-use change (Codron et al., 2012). They can also provide critical information to aid conservationists in developing strategies to manage the ever-increasing problem of elephant-human conflict in Asia and Africa (Hoare, 1999; Naughton-Treves, 1998; Sitati et al., 2003).

Isotopic profiles from unaltered bioapatite in fossil proboscidean tusks could address questions related to seasonality of vegetation, precipitation, and diet in deep time. This will first require careful screening of tusk bioapatite for diagenesis by X-Ray diffraction or other methods to determine feasibility of isotope analysis (Ayliffe et al., 1994). Primary isotope signatures have been recovered from numerous late Pleistocene tusks from North American and Eurasian localities on the order of 10,000 years old at annual to sub-annual scale (Fox et al., 2007; Koch et al., 1989; Rountrey et al., 2012), but isotope profiles on fossil tusks at the weekly resolution we use here have yet to be done. If possible, they have the potential to address questions related to seasonal diet, ecological, and climate variability.

One especially important question with respect to intra-annual climate and ecological variability in East Africa in the geologic past pertains to resource availability for hominins. The frequency (and magnitude) of wet seasons would have had a significant effect on water avail-

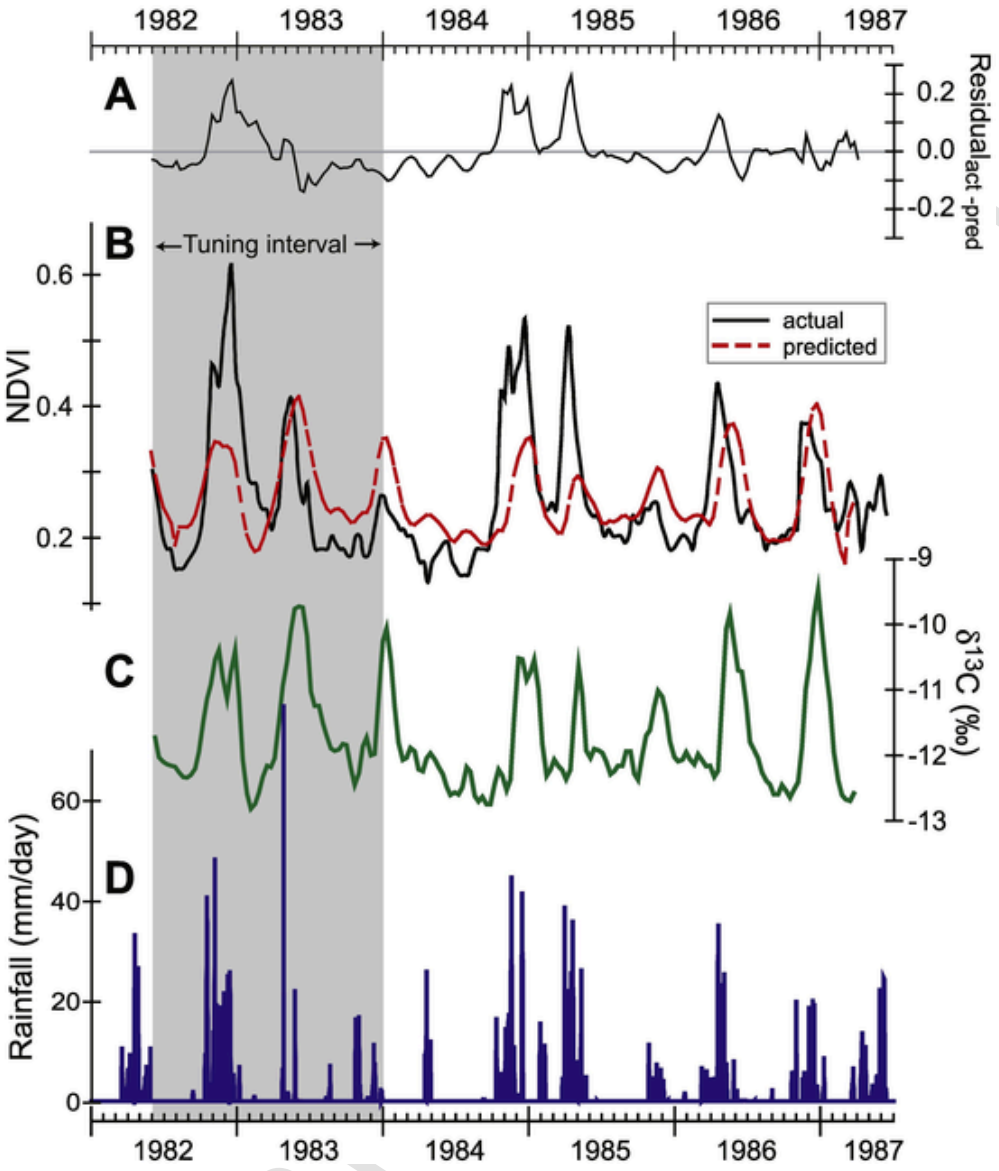

Fig. 11. Matching filter results for predicted Normalized Difference Vegetation Index based on $\delta^{13}C$ (VPDB) data compared to actual NDVI data from 1982 to 1987. A) Residual between actual and predicted NDVI, B) actual (black) vs. predicted (red dashed) NDVI, C) $\delta^{13}C$ that served as matching filter input, and D) rainfall. The shaded box represents the 600-day tuning interval. Rainfall data were collected at Archer's Post by the East African Meteorological Department. (For interpretation of the references to colour in this figure legend, the reader is referred to the web version of this article.)

ability, vegetation structure, and access to food for hominins throughout the year. Whether or not Plio-Pliestocene fossil tusks from East Africa or other parts of the world are suitable for stable isotope profiles remains to be tested. If diagenesis precludes the use of Plio-Pliestocene fossil tusks from East Africa, isotope profiles from proboscidean enamel or other large herbivore molar teeth may provide alternative proxies for examining seasonal environmental variability (Reid et al., 2019; Uno et al., 2020; Yang et al., 2020).

6. Conclusions

The tusk dentin and tail hair profiles from R37 offer a unique opportunity to ground-truth stable isotope data with rainfall, NDVI, GPS location, and observational data. Previous studies utilizing isotope profiles in fossil or modern tusks have all been in environments with annual seasonal cyclicity. We demonstrate that diet and climatic information can be reconstructed at approximately weekly resolution from serially sampled tusk dentin and thus provide a record of seasonal changes in rainfall, vegetation, and diet in ecosystems where C_4 grasses are the dominant grass type. Three methods for measuring tusk growth show excellent agreement, varying by less than 10%. Although tusk growth rate is variable over annual timescales and longer, tuned growth rates differed by $<7\%$ from untuned rates, and we therefore suggest tuning is not necessary. Combined, the isotope profile and growth rate results set the stage for using tusks from the recent geologic record as high-resolution archives of proboscidean life history, terrestrial ecology and paleoclimate. The least squares inverse filter data show that $\delta^{13}C$ can be used to predict NDVI given the appropriate training interval length. Further developed, this may be able to provide quantitative or relative estimates of seasonal vegetation or precipitation changes in ancient environments.

Tusk and hair isotope profile results have several implications for modern elephant ecology. The $\delta^{13}C_{dentin}$ and $\delta^{13}C_{hair}$ profiles from 2000 to 2006 are similar in their magnitude of variation and virtually identical in their ability to record high-frequency changes in diet. Subtle differences may provide insight into physiological processes or nutritional status. Together, the $\delta^{18}O_{dentin}$ and GPS data indicate that during

the wet season, elephants spend less time visiting permanent water sources and instead obtain a higher fraction of their body water from plant water. The $\delta^{15}N_{hair}$ data, in combination with $\delta^{13}C_{hair}$, $\delta^{13}C_{plant}$, and $\delta^{15}N_{plant}$ data, suggest that periods of decoupling in the usual positive relationship between $\delta^{15}N_{hair}$ and $\delta^{13}C_{hair}$ are indicative of diet or metabolic change. R37 and her family, the Swahilis, held a relatively low social rank in the Reserves. Comparison of R37's tusk dentin profile with hair isotope profiles from the Royals, the dominant family unit in the Reserves, indicate different water-use strategies during the wet season that may be related to social rank, demonstrating that comparison of isotope profiles may be a powerful tool for studying social dynamics in ecosystems.

Declaration of Competing Interest

The authors declare that they have no known competing financial interests or personal relationships that could have appeared to influence the work reported in this paper.

Acknowledgements

We thank the Office of the President of the Republic of Kenya, the Kenya Wildlife Service, and the Samburu and Buffalo Springs County Councils for permission to conduct this research. We thank David Daballen, Daniel Lentipo, and Chris Leadismo at Save The Elephants for sample collection; Dan Davis, Blake Hethmon, and Jared Singer for assistance with sample preparation and analyses; and Adam Rountrey for furnishing a copy of the ImageJ plug-in (IncMeas v1.2) used to measure growth increments. We thank Dr. Jessica Metcalfe and two anonymous reviewers for comments that improved this manuscript. This project was supported by National Science Foundation grant EAR-0819611 awarded to Thure Cerling, by a University of Utah Graduate Research Fellowship (KTU), and the Vetlesen Foundation (KTU). Stable isotope analyses were done at the SIRFER facility at the University of Utah. This work was carried out under CITES permits US831854/9, 02US053837/9, and 07US159997/9. This is Lamont-Doherty Earth Observatory contribution #8435.

Appendix A. Supplementary data

Supplementary data to this article can be found online at https://doi.org/10.1016/j.palaeo.2020.109962.

References

Ambrose, S H, Norr, L, 1993. Experimental evidence for the relationship of the carbon isotope ratios of whole diet and dietary protein to those of bone collagen and carbonate. In: Lambert, J B, Grupe, G (Eds.), Prehistoric Human Bone: Archaeology at the Molecular Level. Springer-Verlag, New York, pp. 1–37.

Ayliffe, L, Chivas, A, Leakey, M, 1994. The retention of primary oxygen isotope compositions of fossil elephant skeletal phosphate. Geochim. Cosmochim. Acta 58, 5291–5298.

Ayliffe, L, Cerling, T, Robinson, T, West, A, Sponheimer, M, Passey, B, Hammer, J, Roeder, B, Dearing, M, Ehleringer, J, 2004. Turnover of carbon isotopes in tail hair and breath CO 2 of horses fed an isotopically varied diet. Oecologia 139, 11–22.

Bowen, G J, Wassenaar, L I, Hobson, K A, 2005. Global application of stable hydrogen and oxygen isotopes to wildlife forensics. Oecologia 143, 337–348.

Cerling, T, Harris, J, 1999. Carbon isotope fractionation between diet and bioapatite in ungulate mammals and implications for ecological and paleoecological studies. Oecologia 120, 347–363.

Cerling, T E, Passey, B H, Ayliffe, L K, Cook, C S, Ehleringer, J R, Harris, J M, Dhidha, M B, Kasiki, S M, 2004. Orphans' tales: seasonal dietary changes in elephants from Tsavo National Park, Kenya. Palaeogeogr. Palaeoclimatol. Palaeoecol. 206, 367–376.

Cerling, T E, Wittemyer, G, Rasmussen, H B, Vollrath, F, Cerling, C E, Robinson, T J, Douglas-Hamilton, I, 2006. Stable isotopes in elephant hair document migration patterns and diet changes. Proc. Natl. Acad. Sci. U. S. A. 103, 371–373.

Cerling, T E, Ayliffe, L K, Dearing, M D, Ehleringer, J R, Passey, B H, Podlesak, D W, Torregrossa, A M, West, A G, 2007. Determining biological tissue turnover using stable isotopes: the reaction progress variable. Oecologia 151, 175–189.

Cerling, T E, Wittemyer, G, Ehleringer, J R, Remien, C H, Douglas-Hamilton, I, 2009. History of Animals using Isotope Records (HAIR): a 6-year dietary history of one family of African elephants. Proc. Natl. Acad. Sci. 106, 8093–8100.

Cerling, T E, Harris, J M, Leakey, M G, Passey, B H, Levin, N E, 2010. Stable carbon and oxygen isotopes in East African mammals: modern and fossil. In: Werdelin, L, Sanders, W (Eds.), Cenozoic Mammals of Africa. University of California Press, Berkeley, pp. 941–952.

Cernusak, L A, Barbour, M M, Arndt, S K, Cheesman, A W, English, N B, Feild, T S, Helliker, B R, Holloway-Phillips, M M, Holtum, J A M, Kahmen, A, McInerney, F A, Munksgaard, N C, Simonin, K A, Song, X, Stuart-Williams, H, West, J B, Farquhar, G D, 2016. Stable isotopes in leaf water of terrestrial plants. Plant Cell Environ. 39, 1087–1102.

Cherney, M D, Fisher, D C, Rountrey, A N, 2017. Tusk pairs in the Ziegler reservoir mastodon (*Mammut americanum*) assemblage: implications for site taphonomy and stratigraphy. Quat. Int. 443, 168–179.

Codron, J, Codron, D, Sponheimer, M, Kirkman, K, Duffy, K J, Raubenheimer, E J, Mélice, J L, Grant, R, Clauss, M, Lee-Thorp, J A, 2012. Stable isotope series from elephant ivory reveal lifetime histories of a true dietary generalist. Proc. R. Soc. B Biol. Sci. 2012, 1–9 published online February 15.

Codron, J, Kirkman, K, Duffy, K J, Sponheimer, M, Lee-Thorp, J A, Ganswindt, A, Clauss, M, Codron, D, 2013. Stable isotope turnover and variability in tail hairs of captive and free-ranging African elephants (*Loxodonta africana*) reveal dietary niche differences within populations. Can. J. Zool. 91, 124–134.

Darimont, C T, Reimchen, T E, 2002. Intra-hair stable isotope analysis implies seasonal shift to salmon in gray wolf diet. Can. J. Zool. 80, 1638–1642.

DeNiro, M J, Epstein, S, 1978. Influence of diet on the distribution of carbon isotopes in animals. Geochim. Cosmochim. Acta 42, 495–506.

DeNiro, M J, Epstein, S, 1981. Influence of diet on the distribution of nitrogen isotopes in animals. Geochim. Cosmochim. Acta 45, 341–351.

Douglas-Hamilton, I, 1998. Tracking elephants using GPS technology. Pachyderm 25, 81–92.

Douglas-Hamilton, I, Krink, T, Vollrath, F, 2005. Movements and corridors of African elephants in relation to protected areas. Naturwissenschaften 92, 158–163.

Ehleringer, J R, Bowen, G J, Chesson, L A, West, A G, Podlesak, D W, Cerling, T E, 2008. Hydrogen and oxygen isotope ratios in human hair are related to geography. Proc. Natl. Acad. Sci. 105, 2788–2793.

Elliott, J C, 2002. Calcium phosphate biominerals. In: Kohn, M J, Rakovan, J, Hughes, J (Eds.), Phosphates-Geochemical, Geobiological, and Materials Importance. The Mineralogical Society of America, Chantilly, pp. 427–453.

Fisher, D C, 1987. Mastodon procurement by paleoindians of the Great Lakes region: hunting or scavenging? In: Nitecki, M H, Nitecki, D V (Eds.), The Evolution of Human Hunting. Plenum, New York, pp. 309–421.

Fisher, D C, 1996. Extinction of proboscideans in North America. In: Shoshani, J, Tassy, P (Eds.), The Proboscidea: Evolution and Palaeoecology of Elephants and their Relatives. Oxford University Press, Oxford, pp. 296–315.

Fisher, D C, 2001. Season of death, growth rates, and life history of North American mammoths. In: Proceedings of the International Conference on Mammoth Site Studies. pp. 121–135.

Fisher, D C, 2008. Taphonomy and paleobiology of the Hyde Park mastodon. Palaeontogr. Am. 61, 197–289.

Fisher, D C, Fox, D L, 2003. Season of death and terminal growth histories of Hiscock mastodons. Bull. Buffalo Soc. Nat. Sci. 37, 83–101.

Fisher, D C, Fox, D L, 2007. Season of death of the Dent Mammoths. In: Brunswig, R H, Pitblado, B L (Eds.), From the Dent Prairie to the Peaks of the Rockies: Recent Paleoindian Research in Colorado. University of Colorado Press, Boulder, pp. 123–153.

Fisher, D C, Fox, D L, Agenbroad, L D, 2003. Tusk growth rate and season of death of mammuthus columbi from hot Springs, South Dakota, USA. Deinsea (Rotterdam) 117–133.

Fox, D L, Fisher, D C, 2004. Dietary reconstruction of Miocene Gomphotherium (Mammalia, Proboscidea) from the Great Plains region, USA, based on the carbon isotope composition of tusk and molar enamel. Palaeogeogr. Palaeoclimatol. Palaeoecol. 206, 311–335.

Fox, D L, Fisher, D C, Vartanyan, S, Tikhonov, A N, Mol, D, Buigues, B, 2007. Paleoclimatic implications of oxygen isotopic variation in late Pleistocene and Holocene tusks of mammuthus primigenius from Northern Eurasia. Quat. Int. 169, 154–165.

Gannes, L Z, Del Rio, C M, Koch, P, 1998. Natural abundance variations in stable isotopes and their potential uses in animal physiological ecology. Comp. Biochem. Physiol. A Mol. Integr. Physiol. 119, 725–737.

Hoare, R, 1999. Determinants of human–elephant conflict in a land-use mosaic. J. Appl. Ecol. 36, 689–700.

Hobson, K A, 1999. Tracing origins and migration of wildlife using stable isotopes: a review. Oecologia 120, 314–326.

Ihwagi, F W, Wang, T, Wittemyer, G, Skidmore, A K, Toxopeus, A G, Ngene, S, King, J, Worden, J, Omondi, P, Douglas-Hamilton, I, 2015. Using poaching levels and elephant distribution to assess the conservation efficacy of private, communal and government land in northern Kenya. PLoS One 10, e0139079.

Koch, P L, Fisher, D C, Dettman, D, 1989. Oxygen isotope variation in the tusks of extinct proboscideans: a measure of season of death and seasonality. Geology 17, 515–519.

Kohn, M J, 1996. Predicting animal δ18O: accounting for diet and physiological adaptation. Geochim. Cosmochim. Acta 60, 4811–4829.

Laws, R, 1966. Age criteria for the African elephant, Loxodonta *A. africana*. East Afr. Wildl. J. 4, 1–37.

Lee, P C, Sayialel, S, Lindsay, W K, Moss, C J, 2012. African elephant age determination from teeth: validation from known individuals. Afr. J. Ecol. 50, 9–20.

Lee-Thorp, J A, Sealy, J C, Van Der Merwe, N J, 1989. Stable carbon isotope ratio differences between bone collagen and bone apatite, and their relationship to diet. J. Archaeol. Sci. 16, 585–599.

LeGeros, R, Trautz, O, Klein, E, LeGeros, J, 1969. Two types of carbonate substitution in the apatite structure. Cell. Mol. Life Sci. 25, 5–7.

Levin, N E, Cerling, T E, Passey, B H, Harris, J M, Ehleringer, J R, 2006. A stable isotope aridity index for terrestrial environments. Proc. Natl. Acad. Sci. U. S. A. 93, 11201–11205.

Menke, W, 1989. Geophysical Data Analysis: Discrete Inverse Theory. Academic Press, San Diego.

Metcalfe, J Z, 2018. Pleistocene hairs: microscopic examination prior to destructive analysis. PaleoAmerica 4, 16–30.

Metcalfe, J Z, Longstaffe, F J, Zazula, G D, 2010. Nursing, weaning, and tooth development in woolly mammoths from Old Crow, Yukon, Canada: Implications for Pleistocene extinctions. Palaeogeogr. Palaeoclimatol. Palaeoecol. 298, 257–270.

Naughton-Treves, L, 1998. Predicting patterns of crop damage by wildlife around Kibale National Park, Uganda. Conserv. Biol. 12, 156–168.

Newsome, S D, Tinker, M T, Monson, D H, Oftedal, O T, Ralls, K, Staedler, M M, Fogel, M L, Estes, J A, 2009. Using stable isotopes to investigate individual diet specialization in California sea otters (*Enhydra lutris nereis*). Ecology 90, 961–974.

Nicholson, S E, 2018. The ITCZ and the Seasonal Cycle over Equatorial Africa. Bull. Am. Meteorol. Soc. 99, 337–348.

Nyquist, H, 1928. Certain topics in telegraph transmission theory. Trans. Am. Inst. Electr. Eng. 47, 617–644.

Park, R, Epstein, S, 1960. Carbon isotope fractionation during photosynthesis. Geochim. Cosmochim. Acta 21, 110–126.

Passey, B, Robinson, T, Ayliffe, L, Cerling, T, Sponheimer, M, Dearing, M, Roeder, B, Ehleringer, J, 2005. Carbon isotope fractionation between diet, breath CO2, and bioapatite in different mammals. J. Archaeol. Sci. 32, 1459–1470.

Pettorelli, N, Vik, J O, Mysterud, A, Gaillard, J-M, Tucker, C J, Stenseth, N C, 2005. Using the satellite-derived NDVI to assess ecological responses to environmental change. Trends Ecol. Evol. 20, 503–510.

Podlesak, D W, Torregrossa, A-M, Ehleringer, J R, Dearing, M D, Passey, B H, Cerling, T E, 2008. Turnover of oxygen and hydrogen isotopes in the body water, CO2, hair, and enamel of a small mammal. Geochim. Cosmochim. Acta 72, 19–35.

Reid, R E, Jones, M, Brandt, S, Bunn, H, Marshall, F, 2019. Oxygen isotope analyses of ungulate tooth enamel confirm low seasonality of rainfall contributed to the African humid period in somalia. Palaeogeogr. Palaeoclimatol. Palaeoecol. 534, 109272.

Rountrey, A N, 2009. Life Histories of Juvenile Woolly Mammoths from Siberia: Stable Isotope and Elemental Analyses of Tooth Dentin. University of Michigan, Ann Arbor, MI, USA.

Rountrey, A N, Fisher, D C, Vartanyan, S, Fox, D L, 2007. Carbon and nitrogen isotope analyses of a juvenile woolly mammoth tusk: evidence of weaning. Quat. Int. 169, 166–173.

Rountrey, A N, Fisher, D C, Tikhonov, A N, Kosintsev, P A, Lazarev, P A, Boeskorov, G, Buigues, B, 2012. Early tooth development, gestation, and season of birth in mammoths. Quat. Int. 255, 196–205.

Secord, R, Bloch, J I, Chester, S G B, Boyer, D M, Wood, A R, Wing, S L, Kraus, M J, McInerney, F A, Krigbaum, J, 2012. Evolution of the earliest horses driven by climate change in the Paleocene-Eocene thermal maximum. Science 335, 959–962.

Sikes, S K, 1971. The Natural History of the African Elephant. Cambridge Univ Press.

Sitati, N W, Walpole, M J, Smith, R J, Leader-Williams, N, 2003. Predicting spatial aspects of human–elephant conflict. J. Appl. Ecol. 40, 667–677.

Tieszen, L, Fagre, T, 1993. Effect of diet quality and composition on the isotopic composition of respiratory CO2, bone collagen, bioapatite, and soft tissues. In: Lambert, J B, Grupe, G (Eds.), Prehistoric Human Bone: Archaeology at the Molecular Level. Springer-Verlag, Berlin, pp. 121–155.

Tieszen, L L, Senyimba, M M, Imbamba, S K, Troughton, J H, 1979. The distribution of C3 and C4 grasses and carbon isotope discrimination along an altitudinal and moisture gradient in Kenya. Oecologia 37, 337–350.

Tieszen, L L, Boutton, T W, Tesdahl, K, Slade, N A, 1983. Fractionation and turnover of stable carbon isotopes in animal tissues: implications for δ 13 C analysis of diet. Oecologia 57, 32–37.

Uno, K T, Quade, J, Fisher, D C, Wittemyer, G, Douglas-Hamilton, I, Andanje, S, Omondi, P, Litoroh, M, Cerling, T E, 2013. Bomb-curve radiocarbon measurement of recent biologic tissues and applications to wildlife forensics and stable isotope (paleo) ecology. Proc. Natl. Acad. Sci. 110, 11736–11741.

Uno, K T, Fisher, D, Wittemyer, G, Douglas-Hamilton, I, Carpenter, N, Cerling, T E, 2020. Forward and inverse methods for extracting climate and diet information from stable isotope profiles in proboscidean molars. Quat. Int.. doi:10.1016/j.quaint.2020.06.030.

Williams, R A D, Elliott, J C, 1979. Basic and Applied Dental Biochemistry. Churchill Livingstone, Edinburgh.

Wittemyer, G, 2001. The elephant population of Samburu and Buffalo Springs national reserves, Kenya. Afr. J. Ecol. 39, 357–365.

Wittemyer, G, Getz, W M, 2007. Hierarchical dominance structure and social organization in African elephants, *Loxodonta africana*. Anim. Behav. 73, 671–681.

Wittemyer, G, Getz, W, Vollrath, F, Douglas-Hamilton, I, 2007. Social dominance, seasonal movements, and spatial segregation in African elephants: a contribution to conservation behavior. Behav. Ecol. Sociobiol. 61, 1919–1931.

Wittemyer, G, Polansky, L, Douglas-Hamilton, I, Getz, W M, 2008. Disentangling the effects of forage, social rank, and risk on movement autocorrelation of elephants using Fourier and wavelet analyses. Proc. Natl. Acad. Sci. 105, 19108–19113.

Wittemyer, G, Cerling, T E, Douglas-Hamilton, I, 2009. Establishing chronologies from isotopic profiles in serially collected animal tissues: an example using tail hairs from African elephants. Chem. Geol. 267, 3–11.

Wittemyer, G, Daballen, D, Douglas-Hamilton, I, 2013. Comparative demography of an at-risk African elephant population. PLoS One 8, e53726.

Yang, D, Uno, K T, Souron, A, McGrath, K, Pubert, E, Cerling, T E, 2020. Intra-tooth stable isotope variations in warthog canines and third molars: implications for paleoenvironmental reconstruction. Chem. Geol.. doi:10.1016/j.chemgeo.2020.119799.

Zazzo, A, Bocherens, H, Brunet, M, Beauvilain, A, Billiou, D, Mackaye, H T, Vignaud, P, Mariotti, A, 2000. Herbivore paleodiet and paleoenvironmental changes in Chad during the Pliocene using stable isotope ratios of tooth enamel carbonate. Paleobiology 26, 294–309.